

**Analysis of M-ary Rectangular Quadrature Amplitude Modulation
(QAM) and A New Blind Equalization Algorithm (Rectangular
Contour Algorithm) Using Rectangular QAM**

By

Qasim Umar Khan
MS-59-09-306 (EE)
2009-NUST-MS PhD-Elec-06



Submitted to the Department of Electrical Engineering
in Partial Fulfillment of the requirements for the Degree of

Master of Science
in
Electrical Engineering

Thesis Advisor

Dr. Shahzad Amin Sheikh

College of Electrical & Mechanical Engineering

National University of Sciences and Technology, Pakistan

2011



The wireless communication has developed enormously in past five decades in terms of high data rates, security, reliability, installation times and cost of cabling. It provides a new level of flexibility or system design, reconfiguration and agility. The wireless technology is very common in our daily life e.g. the use of cellular phone, wireless internet etc. The most recent research is based on wireless technology for providing broadband communication to high speed vehicles. The processing power of the digital hardware plays important role in this success of wireless communication which now makes it possible to implement sophisticated algorithms achieving better performance and high data rates. The transmitted signal suffers with the impairments introduced by wireless channels. These impairments include frequency selectivity, time selectivity and noise. The channel needs to be estimated or equalized for the coherent detection of the transmitted signal. Channel equalization and channel estimation is used in this regard depending on the system model and feasibility. Orthogonal Frequency Division Multiplexing (OFDM) which is multi carrier communication system employs estimation because of the one to one relationship between the transmitted and received signal. After the estimation, simple channel inversion can retrieve the transmitted signal. On the other hand Single Carrier (SC) communication uses channel equalization. The equalizer is a transversal filter which tries to approximate an inverse channel so that it nullifies the effect of the channel when the received data passes through it. The ultimate goal of these techniques is to try to estimate or equalize within overhead, processing power and time.

Different types of equalization techniques exist including Data Aided and blind equalization. The data aided schemes use training data while blind equalizers don't use training data rather they depend upon the signal constellations and channel statistics. Data aided schemes take relatively less time to converge to the solution. These are imperative in presence of high time selectivity (less coherence time or more Doppler spread) in which periodic transmission of training is used to track the variations of the channel. On the other hand, blind equalizers are generally used in situations where the channel remains constant for relatively longer periods of time and changes very slowly (low Doppler spread). The blind equalizer/estimators take relatively more time to converge to the solution. These are usually employed in scenarios

where delays in the start up time do not matter much and users are static, e.g. Digital Audio and Video Broadcasting, surveillance applications, asynchronous transfer mode (ATM), local area network (LAN), broadband access on copper in fiber-to-the-curb (FTTC) and very high-rate digital subscriber line (VDSL) networks.[1]-[3].

The transmitted signal is formed of bits mapped on constellations to be used for the modulation/demodulation. Different types of modulation schemes exist e.g. Pulse Amplitude Modulation (PAM). Phase Shift Keying (PSK), Quadrature Amplitude Modulation (QAM) etc. QAM has been widely used in digital communication systems due to its high bandwidth efficiency. When the number of bits per symbol is even, transmission can be implemented easily by using square QAM. However, when the transmitted symbol statistics are of quadrature amplitude modulation (QAM) non-square constellations for which the number of bits per symbol is odd, the N -points constellations ($N = 2^{2i+1}$, i Integer and $i \geq 0$) can be arranged into Cross QAM given by Smith [4] and Rectangular QAM (RQAM) constellations so long as $E[s_R^2(n)] \neq E[s_I^2(n)]$ is satisfied. The use of RQAM in equalization [5] shows that it provide faster convergence rate due to its ability of correcting any phase error within 180° . This is because the four saddle points existing in the square and cross constellations along $\theta(k) = \frac{\pi}{4}, \frac{3\pi}{4}, \frac{5\pi}{4}, \frac{7\pi}{4}$ are absent when using RQAM. Consequently, the frequency of being attracted toward the vicinity of the saddle points, around which it exhibits slow convergence, before converging to the desired minimum, is significantly diminished when using RQAM. Therefore, the use of RQAM may accelerate the magnitude equalization process during the transient operation.

Current focus of the research in the blind equalization schemes is to develop such algorithms that minimum time to converge and at the same time require less computational power. Also the existing algorithms for blind equalization are based on mostly using Square QAM e.g. Square Contour Algorithm (SCA), Improved SCA etc and Cross QAM e.g. Modified Multi Modulus Algorithm (MMMA), Generalized Cross Contour Algorithm (GCrCA) etc and modifications have been done on these algorithms to provide better performance and also to be used for RQAMs, however no such algorithm to best of my knowledge specifically for RQAM using odd number of bits per symbols exists, thus this is the first motivation for the thesis to develop the algorithm which is based on RQAM thus providing faster convergence

rate as can be seen through simulation results over the existing algorithm using Cross QAM (GCrCA) [6] or RQAM (MMA) [5].

The existing blind equalization algorithms are mostly QAM specific e.g. SCA, ISCA works best with Square QAM. On the other hand, MMMA, GCrCA works best for the Cross QAM. To best of my knowledge no algorithm performs well simultaneously for both types of QAM, thus motivating for the development of the algorithm that performs well for both types of QAMs. This is the second motivation for the thesis. To develop such algorithm that provide ease in implementation, RQAM and constellation parameters are used, the detail of which is provided in the coming chapters. This algorithm is named as Rectangular Contour Algorithm ($R_{RECT}CA$). The tool used for the simulation purpose is MATLAB. The performance of the algorithm has been tested and verified through simulations on MATLAB.

The proposed algorithm provide better convergence rate, low steady state error and less computational complexity as compared to MMA, GCrCA.

The rest of the thesis has been organized as follows:

Chapter 2 discusses the concept of QAM constellations, their analysis in general and in particular analysis of RQAM in terms of average energy and symbol error probability SEP over AWGN and fading channels including Rayleigh, Nakagami-m, Nakagami-q (Hoyt) and Nakagami-n (Rice). Chapter 3 describes the concept of blind equalization and major blind equalization algorithms along with system and channel modelling. Chapter 4 describes the $R_{RECT}CA$ and its simulation results and finally there are conclusion and future recommendations.

Chapter 2 QAM CONSTELLATIONS

QAM has been widely used in digital communication systems due to reducing or eliminating inter modulation interference caused by a continuous carrier near the modulation sidebands and its high bandwidth efficiency. Different QAMs exist e.g. Square QAM where number of bits per symbol is even and Cross QAM where number of bits per symbol is odd. The Square QAM and Cross QAM are common and have been thoroughly investigated in terms of symbol error probability, blind equalization techniques etc. In [7] the author has discussed and analysed the Square QAM and Cross QAM in detail in terms of average energy, minimum distance between the symbols in the constellation, symbol error probability (SEP) etc.

2.1 *M*-ary Square QAM (*M*-SQAM)

For Square QAM M is defined as 2^k where k is number of bits per symbol and is even integer ($k \geq 2$) for Square QAM i.e. $M = 4, 16, 64, \dots$. Fig 2.1 shows 16-Square QAM, the average energy required by M -ary Square QAM is given by [7]

$$\varepsilon_{av} = \frac{d^2}{6}(M-1) \quad (1)$$

The SEP expression is

$$P_{SEP} = 4 \left(1 - \frac{1}{\sqrt{M}}\right) Q\left(\frac{d}{2\sigma}\right) - 4 \left(1 - \frac{1}{\sqrt{M}}\right)^2 Q^2\left(\frac{d}{2\sigma}\right) \quad (2)$$

The rest of the expressions derived in terms of equ (1) and equ (2) are summarized in Table.2.1

Parameters	Expressions
Minimum Distance d	$d = \sqrt{\frac{6\epsilon_{av}}{M-1}}$
Average Energy ϵ_{av}	$\epsilon_{av} = \frac{d^2}{6}(M-1)$
Energy per dimension $\bar{\epsilon}_{av}$	$\bar{\epsilon}_{av} = \frac{d^2}{12}(M-1)$
Bit per dimension \bar{k}	$\bar{k} = \frac{1}{2} \log_2 \left(12 \frac{\bar{\epsilon}_{av}}{d^2} + 1 \right)$
Symbol error probability P_{SEP}	$P_{SEP} = 4 \left(1 - \frac{1}{\sqrt{M}} \right) Q \left(\frac{d}{2\sigma} \right) - 4 \left(1 - \frac{1}{\sqrt{M}} \right)^2 Q^2 \left(\frac{d}{2\sigma} \right)$

Table 2.1 Mathematical Expressions for M-SQAM

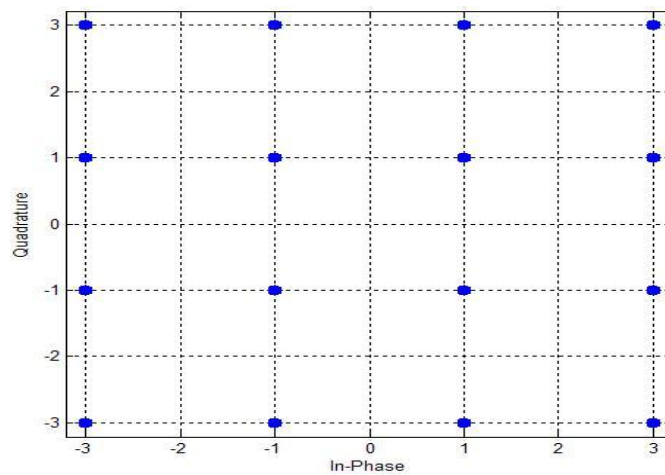


Fig.2.1 16-Square QAM

2.2 M-ary Cross QAM (M-XQAM)

Since in Cross QAM we are dealing with odd number of bits per symbol so we define M as 2^{2k+1} where $k \geq 2$. Fig.2.2 shows 32-Cross QAM. It should be noted here that Cross QAM deal with $M = 8$ as a special case for which separate expressions for average energy, SEP etc are required. The average energy associated with Cross QAM is given by [7] as

$$\varepsilon_{av} = \frac{d^2}{6} \left(\frac{31}{32} M - 1 \right) \quad (3)$$

and SEP as

$$P_{SEP} = 4 \left(1 - \frac{1}{\sqrt{2M}} \right) Q \left(\frac{d}{2\sigma} \right) - 4 \left(1 - \sqrt{\frac{2}{M}} \right)^2 Q^2 \left(\frac{d}{2\sigma} \right) \quad (4)$$

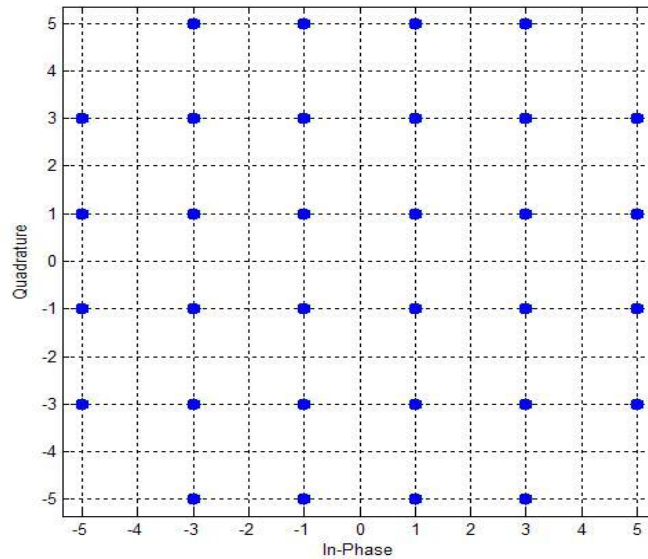


Fig.2.2 32-Cross QAM

Table 2.2 summarizes the rest of expressions in term of equ (3) and equ (4)

Parameters	Expressions
Minimum Distance d	$d = \sqrt{\frac{6\varepsilon_{av}}{\left(\frac{31}{32}\right)^{M-1}}}$
Average Energy ε_{av}	$\varepsilon_{av} = \frac{d^2}{6} \left(\frac{31}{32} M - 1\right)$
Energy per dimension $\bar{\varepsilon}_{av}$	$\bar{\varepsilon}_{av} = \frac{d^2}{12} \left(\frac{31}{32} M - 1\right)$
Bit per dimension \bar{k}	$\bar{k} = \frac{1}{2} \log_2 \left(\frac{32}{31} \left(12 \frac{\bar{\varepsilon}_{av}}{d^2} + 1 \right) \right)$
Symbol error probability P_{SEP}	$P_{SEP} \approx 4 \left(1 - \frac{1}{\sqrt{2M}} \right) Q \left(\frac{d}{2\sigma} \right) - 4 \left(1 - \sqrt{\frac{2}{M}} \right)^2 Q^2 \left(\frac{d}{2\sigma} \right)$

Table 2.2 Mathematical Expressions for M-XQAM

2.3 M-ary Rectangular QAM (M-RQAM)

Rectangular QAM is defined where number of bits per symbol is odd. Fig.2.3 shows 32-Rectangular QAM. M-RQAM is being investigated in the thesis for its utilization in the blind equalization algorithms. However before proceeding to the algorithm, we perform the complete analysis of the Rectangular QAM and verified that the resulting expressions so derived are in excellent agreement with the one found in literature [8]-[10]. The exact expression of SEP of the Rectangular QAM over AWGN and fading channel including, Rayleigh, Nakagami-m, Nakagami-q (Hoyt) and Nakagami-n (Rice) is derived.

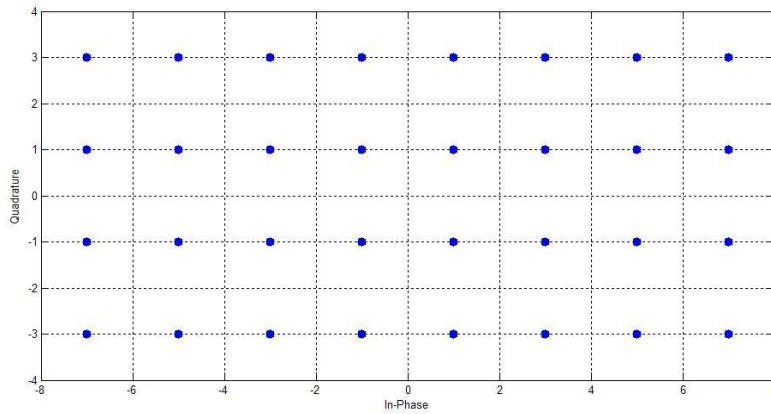


Fig.2.3 32-Rectangular QAM

Since we are dealing with QAMs with odd number of bits per symbol so we again define $M = 2^{2k+1}$ with $k \geq 1$, that is, $M = 8, 32, 128, 512, 2048, \dots$. It is worth noting here that Rectangular QAM deal $k = 1$, $M = 8$ as an ordinary case for which no separate SEP expression is required as compared to Cross QAM which require separate SEP expression. The block parameter for M-RQAM is given as

$$P \triangleq \sqrt{\frac{M}{8}} \quad (5)$$

Thus Rectangular QAM constellation is constructed by $P \times 2P$ rectangular block in each quadrant. According to the symmetry, only first quadrant of general M-RQAM constellation is shown in Fig.2.4.

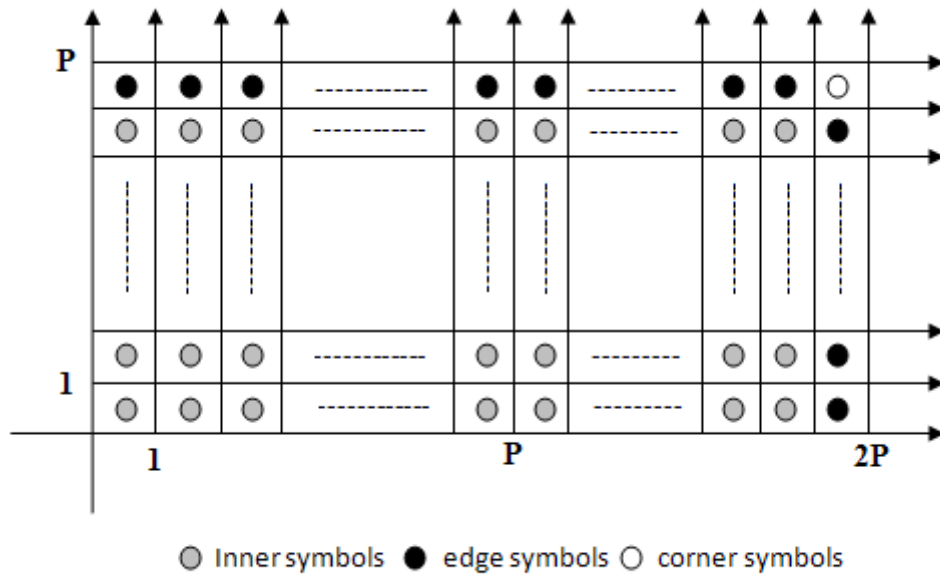


Fig.2.4 First Quadrant of General M-RQAM

It can be seen that optimal decision regions are square where dots represent signal symbols while the lines indicate decision boundaries. There are three types of symbols: inner, corner and edge. According to the symmetry, it is enough to consider the symbols in one quadrant in the Rectangular QAM constellation. The total number of these three types of symbols in M-RQAM are respectively given as

$$\begin{aligned}
 N_{inner} &= \left(2^k - [2^{k-2} + 12] \right) \\
 N_{corner} &= 4 \\
 N_{edge} &= (2^{k-2} + 8)
 \end{aligned} \tag{6}$$

Let d be the minimum Euclidean distance between the adjacent symbols in the constellation, and let $N_0/2$ denote the two-sided power spectral density of zero mean AWGN (i.e. its variance $\sigma^2 = \frac{N_0}{2}$). The exact SEP expressions will be written in terms of the Gaussian

Q-Function

$$Q(x) = \frac{1}{\sqrt{2\pi}} \int_x^\infty e^{-t^2/2} dt \tag{7}$$

and well known integral function related to the alternate representation of one and two dimensional joint Gaussian Q-function [11]-[14]

$$Q_a(x, \varphi) = \frac{1}{2\pi} \int_0^\varphi e^{-\frac{x^2}{2\sin^2\theta}} d\theta, x \geq 0 \quad (8)$$

In particular $Q(x) = Q_a(x, \pi) = 2Q_a(x, \pi/2)$ [12, equation 2] and $Q^2(x) = 2Q_a(x, \pi/4)$ [13 equation 12], both for $x \geq 0$. It should be noted that in addition to the advantage of having finite integration limits, the above function has the argument x contained in the integrand rather than in the integration limits and it also has an integrand that is exponential in the argument x , so that it can be evaluated with more accuracy. Moreover, the above function has some interesting implications with regard to simplifying the evaluation of performance results related to communication problems, for example, the SEP performance evaluation over fading channels, wherein the argument of the Q_a function is dependent on random system parameters and, thus, requires averaging over the statistics of these parameters. The argument x of equ.(7) and equ.(8) is expressed as a multiple of

$$\beta \triangleq \frac{d}{2\sqrt{N_o/2}} \quad (9)$$

which denotes the normalized least distance (in noise standard deviation) from a symbol to an adjacent symbol. Assuming that the signal points are equally probable and according to the symmetry of the constellation, it can be shown that the average symbol energy for Rectangular M-QAM constellation is given by

$$\varepsilon_{av} = \frac{4}{M} \left[P \sum_{m=1}^{2P} \left\{ \left(\frac{d(2m-1)}{2} \right)^2 \right\} + 2P \sum_{n=1}^P \left\{ \left(\frac{d(2n-1)}{2} \right)^2 \right\} \right] = \frac{d^2}{6} \left\{ \frac{10M}{8} - 1 \right\} \quad (10)$$

Since symbol's signal to noise ratio SNR can be written as

$$SNR = \frac{\varepsilon_{av}}{N_o} = \frac{d^2 \left\{ \frac{10M}{8} - 1 \right\}}{6N_o} = \frac{d^2 \left(\frac{\left\{ \frac{10M}{8} - 1 \right\}}{3} \right)}{2N_o} = \frac{\beta^2 \left\{ \frac{10M}{8} - 1 \right\}}{3} \quad (11)$$

Thus $\beta = \sqrt{\frac{3}{\left\{ \frac{10M}{8} - 1 \right\}}} SNR = \sqrt{2DSNR} = \sqrt{2D\gamma}$ where $D = 1.5 / \left\{ \frac{10M}{8} - 1 \right\}$, $SNR = \gamma$

The SEP expressions will be derived in term of β .

2.3.1 Symbol Error Probability in AWGN Channel

Due to independence of quadrature and inphase components the SEP expressions of M-RQAM can easily derived by using the same lines as in [7] therefore probability of correct symbol reception of any inner, corner and edge symbol can be written, respectively, as

$$\begin{aligned} P_{inner} &= (1 - 2Q(\beta))^2 = 1 - 4Q(\beta) + 4Q^2(\beta) \\ P_{corner} &= (1 - Q(\beta))^2 = 1 - 2Q(\beta) + Q^2(\beta) \\ P_{edge} &= (1 - Q(\beta))(1 - 2Q(\beta)) = 1 - 3Q(\beta) + 2Q^2(\beta) \end{aligned} \quad (12)$$

The exact average probability of correctly receiving symbol for M-ary Rectangular QAM is given therefore as

$$\begin{aligned} P_{correct}(\beta) &= \frac{1}{M} \left[N_{inner} P_{inner} + N_{corner} P_{corner} + N_{edge} P_{edge} \right] \\ &= 1 - \frac{15}{4} \left[1 - \frac{64}{15M} \right] Q(\beta) + \frac{7}{2} \left[1 - \frac{8}{M} \right] Q^2(\beta) \end{aligned} \quad (13)$$

Since $P_{SEP} = 1 - P_{correct}$ thus average exact SEP for M-ary Rectangular QAM is given as

$$P_{SEP}(\beta) = \frac{15}{4} \left[1 - \frac{64}{15M} \right] Q(\beta) - \frac{7}{2} \left[1 - \frac{8}{M} \right] Q^2(\beta) \quad (14)$$

Equ.(14) gives the exact SEP expression for M-RQAM. The results in Fig.2.5 through Fig 2.9 confirms that the expression so derived is in complete agreement with the one find in literature using different approaches [8]-[10] and simulations. These figures from 5-9 shows the results for $M = 8, 32, 128, 512, 2048$.

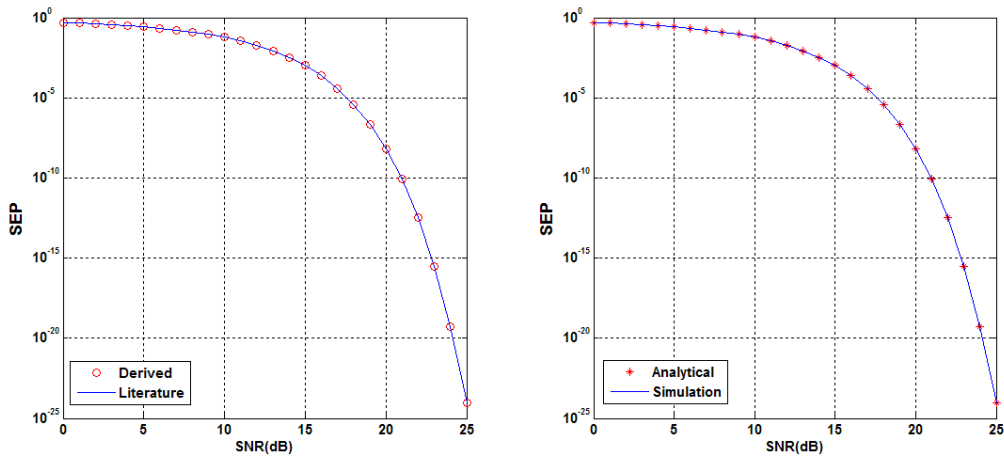


Fig 2.5 Symbol Error Probability of 8-RQAM over AWGN Channel

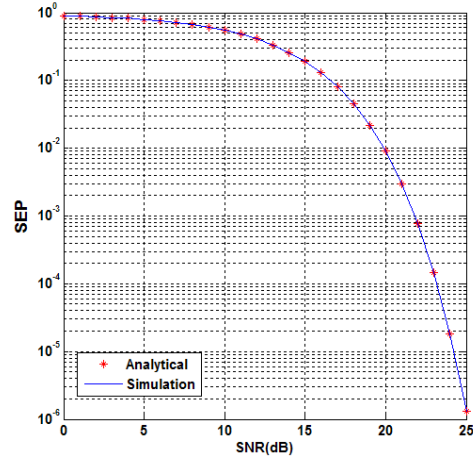
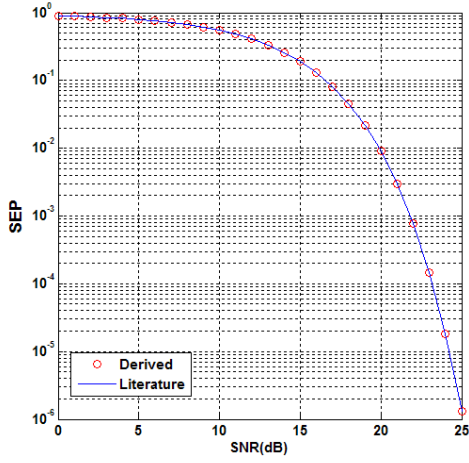


Fig 2.6 Symbol Error Probability of 32-RQAM over AWGN Channel

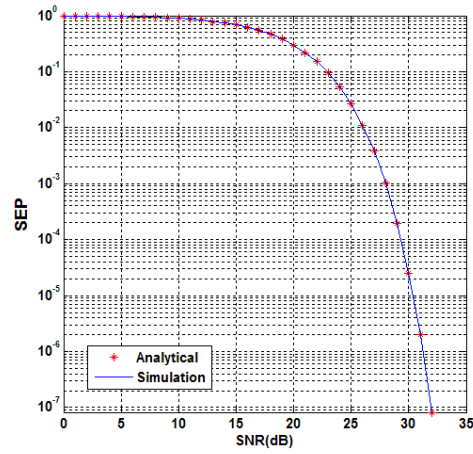
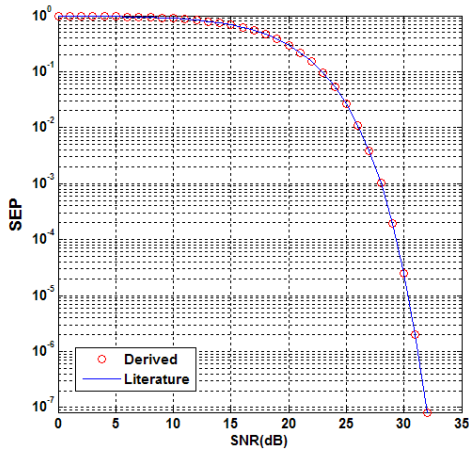


Fig 2.7 Symbol Error Probability of 128-RQAM over AWGN Channel

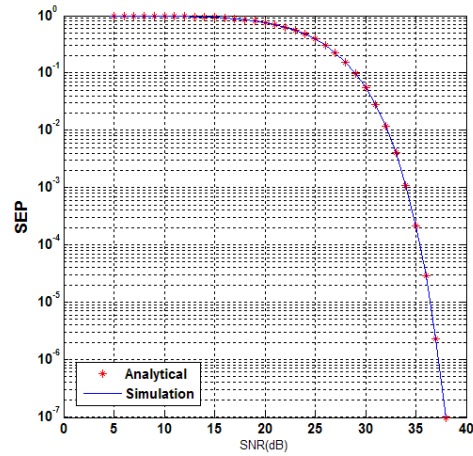
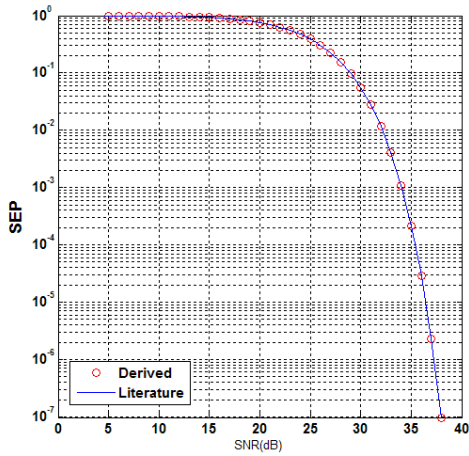


Fig 2.8 Symbol Error Probability of 512-RQAM over AWGN Channel

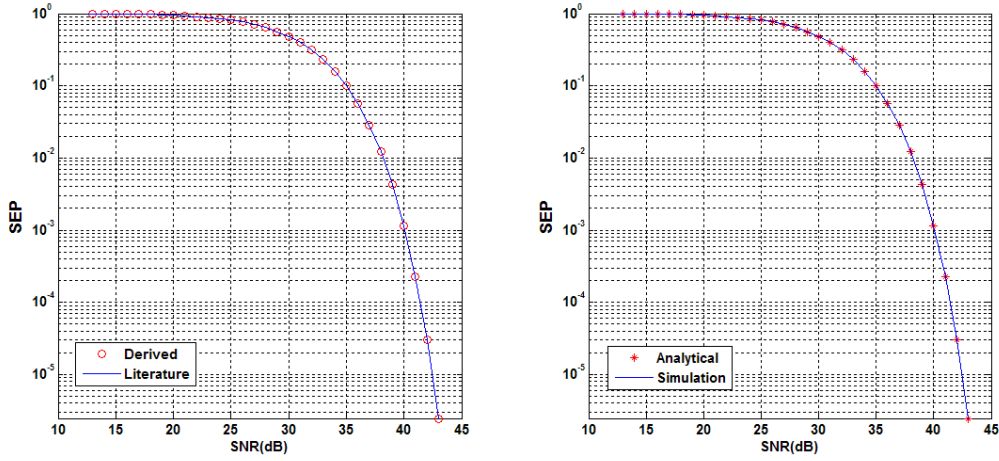


Fig 2.9 Symbol Error Probability of 2048-RQAM over AWGN Channel

2.3.2 Symbols Error Probability in Fading Channels.

The fading channels, including Rayleigh, Nakagami-m, Nakagami-q (Hoyt) and Nakagami-n (Rice) channels are considered. The probability density function (pdf) of the instantaneous received SNR γ in these channels can be written, respectively as [11]

$$\begin{aligned}
 p_{\gamma_R}(\gamma) &= \frac{1}{\Omega} e^{-\frac{\gamma}{\Omega}}, \\
 p_{\gamma_m}(\gamma) &= \frac{m^m \gamma^{m-1}}{\Omega^m \Gamma(m)} e^{-\frac{m}{\Omega} \gamma}, m \geq \frac{1}{2}, \\
 p_{\gamma_q}(\gamma) &= \frac{1+q^2}{2q\Omega} e^{-\frac{(1+q^2)^2}{4q^2\Omega} \gamma} I_0\left(\frac{1-q^4}{4q^2\Omega} \gamma\right), 0 \leq q \leq 1, \\
 p_{\gamma_n}(\gamma) &= \frac{1+K}{\Omega} e^{-K-\frac{1+K}{\Omega} \gamma} I_0\left(2\sqrt{\frac{1+K}{\Omega} K \gamma}\right), K \geq 0
 \end{aligned} \tag{15}$$

where $\gamma = r^2 E_s / N_0$ is the instantaneous SNR of the received symbol, r is the instantaneous fading amplitude of the channel, E_s is the energy of each transmitted symbol, N_0 is the one-sided power spectral density of the zero mean AWGN, $\Omega = E\{\gamma\}$ is the average received SNR per symbol, and $E\{-\}$ denotes the expectation operator. $I_0(-)$ is the modified Bessel

function of the first kind and zeroth order. The moment generator functions MGF $M_\gamma(s) \triangleq E\{e^{-s\gamma}\}$ corresponding to above pdfs are respectively given by [11]

$$\begin{aligned}
M_{\gamma_R}(s) &= (1 + \Omega s)^{-1}, \\
M_{\gamma_m}(s) &= \left(1 + \frac{\Omega}{m} s\right)^{-m}, m \geq \frac{1}{2}, \\
M_{\gamma_q}(s) &= \left(1 + 2\Omega s + \left(\frac{2q\Omega}{1+q^2}\right)^2 s^2\right)^{-1/2}, 0 \leq q \leq 1, \\
M_{\gamma_n}(s) &= \frac{1+K}{1+K+\Omega s} e^{-\frac{K\Omega s}{1+K+\Omega s}}, K \geq 0.
\end{aligned} \tag{16}$$

Averaging the P_{SEP} expression of AWGN over the fading distribution of the received SNR γ , induces the average SEP of arbitrary M-ary Rectangular QAM over fading channel as given by

$$P_{F_SEP} = \int_0^\infty P_{SEP}(\gamma) p_\gamma(\gamma) d\gamma = \frac{15}{4} \left[1 - \frac{64}{15M}\right] I(D, \frac{\pi}{2}) - \frac{7}{2} \left[1 - \frac{8}{M}\right] I(D, \frac{\pi}{4}) \tag{17}$$

where $p_\gamma(\gamma)$ denotes the pdf of γ and $I(D, \varphi) = 2 \int_0^\infty Q_a(\sqrt{2D\gamma}, \varphi) p_\gamma(\gamma) d\gamma$

The relationships $Q(x) = 2Q_a(x, \pi/2)$ and $Q^2(x) = 2Q_a(x, \pi/4)$ for $x \geq 0$ are applied to obtain P_{F_SEP} . It is possible to re-express above integral in terms of MGF of γ as given by

$$\begin{aligned}
I(D, \varphi) &= \int_0^\infty \frac{1}{\pi} \int_0^\varphi \exp\left(-\frac{D\gamma}{\sin^2 \theta}\right) d\theta p_\gamma(\gamma) d\gamma = \int_0^\varphi \frac{1}{\pi} \int_0^\infty \exp\left(-\frac{D\gamma}{\sin^2 \theta}\right) p_\gamma(\gamma) d\gamma d\theta \\
&= \frac{1}{\pi} \int_0^\varphi M_\gamma\left(\frac{D}{\sin^2 \theta}\right) d\theta
\end{aligned} \tag{18}$$

Substituting the MGF of equ.(16) in the equ.(18) , the corresponding expression of $I(D, \varphi)$ of equ.(19) for Rayleigh, Nakagami-m, Nakagami-q (Hoyt) and Nakagami-n (Rice) channels are

$$\begin{aligned}
 I_{\gamma_R}(D, \varphi) &= \frac{1}{\pi} \int_0^\varphi \frac{\sin^2 \theta}{\sin^2 \theta + D\Omega} d\theta, \\
 I_{\gamma_m}(D, \varphi) &= \frac{1}{\pi} \int_0^\varphi \left(1 + \frac{\Omega}{m} \frac{D}{\sin^2 \theta} \right)^{-m} d\theta, \\
 I_{\gamma_q}(D, \varphi) &= \frac{1}{\pi} \int_0^\varphi \left(1 + \frac{2\Omega D}{\sin^2 \theta} + \left(\frac{2q\Omega}{1+q^2} \right)^2 \frac{D^2}{\sin^4 \theta} \right)^{-1/2} d\theta, \\
 I_{\gamma_n}(D, \varphi) &= \frac{1}{\pi} \int_0^\varphi \frac{1+K}{1+K+\Omega D \csc^2 \theta} \exp\left(-\frac{K\Omega D}{(1+K)\sin^2 \theta + \Omega D} \right) d\theta,
 \end{aligned} \tag{19}$$

Using the above four integral expressions, the average SEP equ.(17) over fading channels can be conveniently evaluated through numerical integration since these formulae are single integrals with finite limits and an integrand composed of elementary (exponential, trigonometric, and/or power) functions. The results in Fig.2.10-Fig.2.14 for $M=8,32,128,512,2048$ show that these expression are in an excellent agreement with one found in literature [8]-[10] derived by using different approaches and simulation. For fading channels, the Rayleigh channel is chosen as a special case since the results of the other type channels are similar to that of Rayleigh channel.

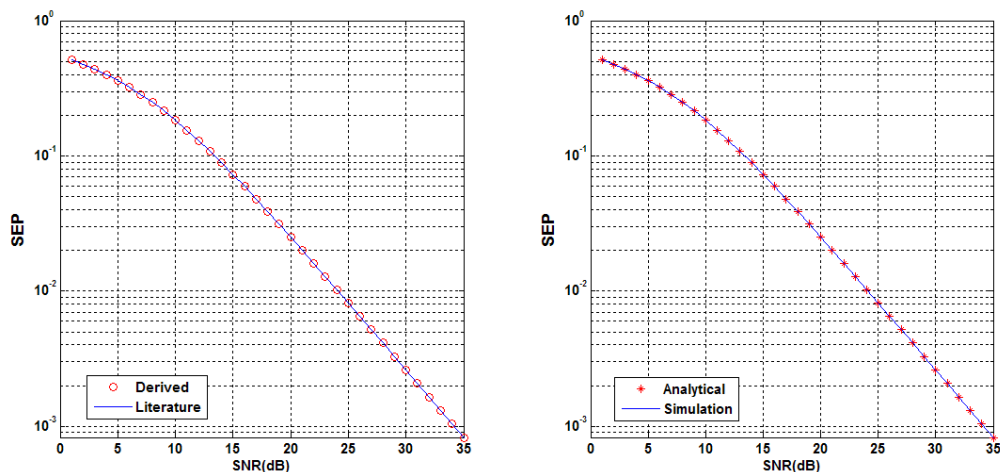


Fig.2.10 Symbol Error Probability of 8-RQAM over Rayleigh Channel

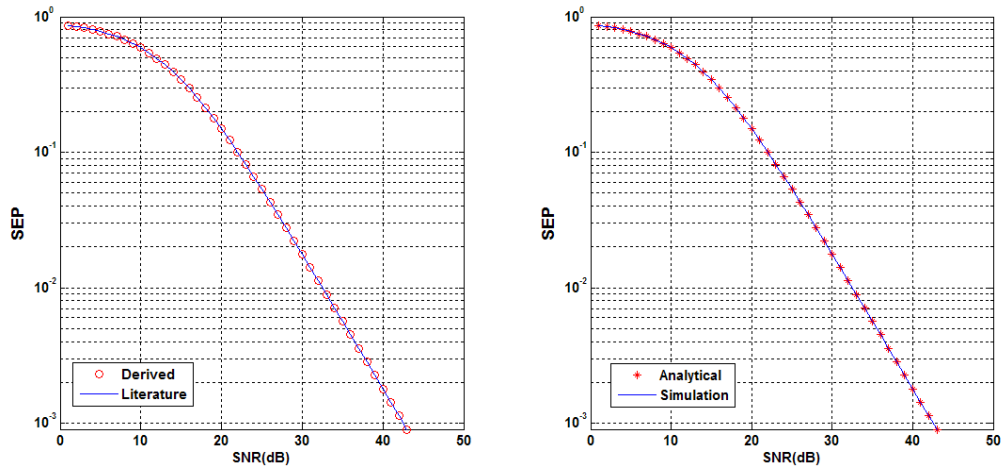


Fig.2.11 Symbol Error Probability of 32-RQAM over Rayleigh Channel

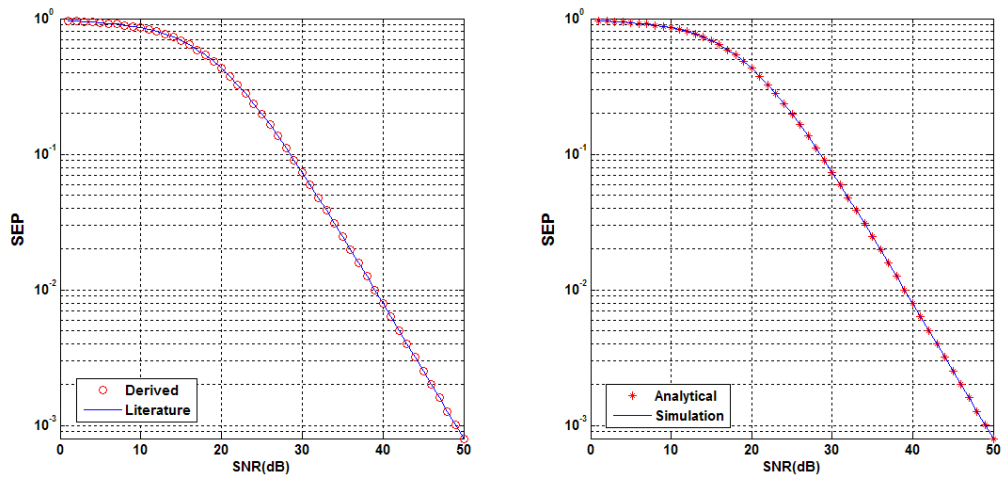


Fig.2.12 Symbol Error Probability of 128-RQAM over Rayleigh Channel

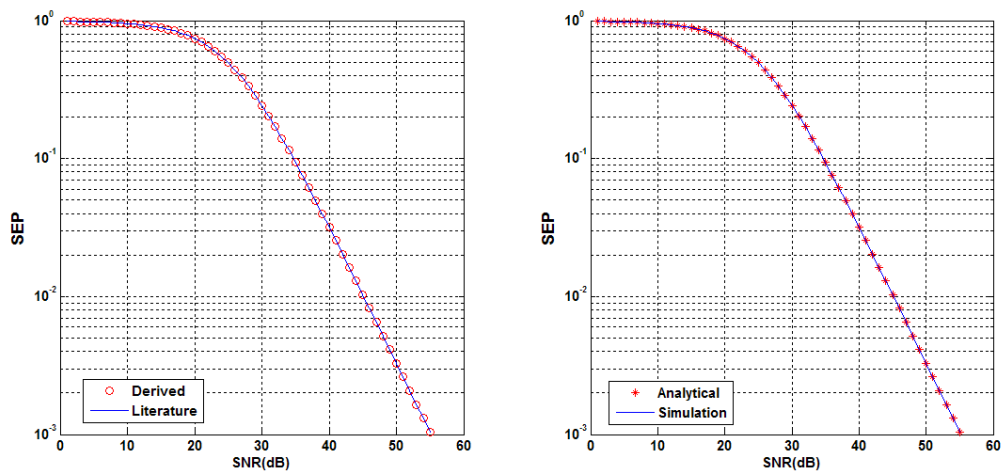


Fig.2.13 Symbol Error Probability of 512-RQAM over Rayleigh Channel

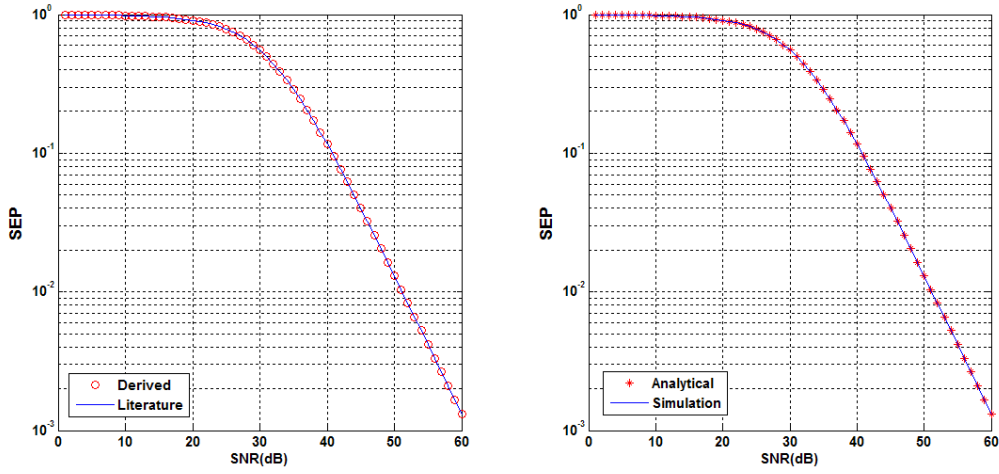


Fig.2.14 Symbol Error Probability of 2048-RQAM over Rayleigh Channel

Table 2.3 summarizes the expressions obtain for the M-RQAM

Parameters	Expressions
Minimum Distance d	$d = \sqrt{\frac{6\varepsilon_{av}}{\left(\frac{10}{8}\right)^M - 1}}$
Average Energy ε_{av}	$\varepsilon_{av} = \frac{d^2}{6} \left\{ \frac{10M}{8} - 1 \right\}$
Energy per dimension $\bar{\varepsilon}_{av}$	$\bar{\varepsilon}_{av} = \frac{d^2}{12} \left\{ \frac{10M}{8} - 1 \right\}$
Bit per dimension \bar{k}	$\bar{k} = \frac{1}{2} \log_2 \left(\frac{8}{10} \left(12 \frac{\varepsilon_{av}}{d^2} + 1 \right) \right)$
Symbol error probability P_{SEP}	$P_{SEP}(\beta) = \frac{15}{4} \left[1 - \frac{64}{15M} \right] Q \left(\frac{d}{2\sigma} \right) - \frac{7}{2} \left[1 - \frac{8}{M} \right] Q^2 \left(\frac{d}{2\sigma} \right)$

Table 2.3 Mathematical Expressions for M-RQAM

2.4 Equal Energy Case:

The problem associated with the M-RQAM is that it requires more average energy than the M-XQAM however this problem can be overcome by reducing the distance between the symbols in the constellation from 2 to 1.75, thus making the average energy almost the same of M-RQAM and M-XQAM, e.g. 32-XQAM with $d = 2$ requires average energy of 20 while 32-RQAM with $d = 1.75$ requires 19.90625 which is almost same as 32-XQAM. It is important to note here that the reducing the d in M-RQAM will not affect its SEP this is because $\sigma = \sqrt{(\epsilon_{av}/2)10^{(-SNR/10)}}$ therefore $\beta = d/\sqrt{(\epsilon_{av}/2)10^{(-SNR/10)}}$ and by equ.(10) increasing d will increase ϵ_{av} and vice versa thereby keeping β approximately the same. Fig.2.15-Fig.2.16 confirms this for $M=8,32,128,512,2048$ for AWGN and Rayleigh Fading channels respectively.

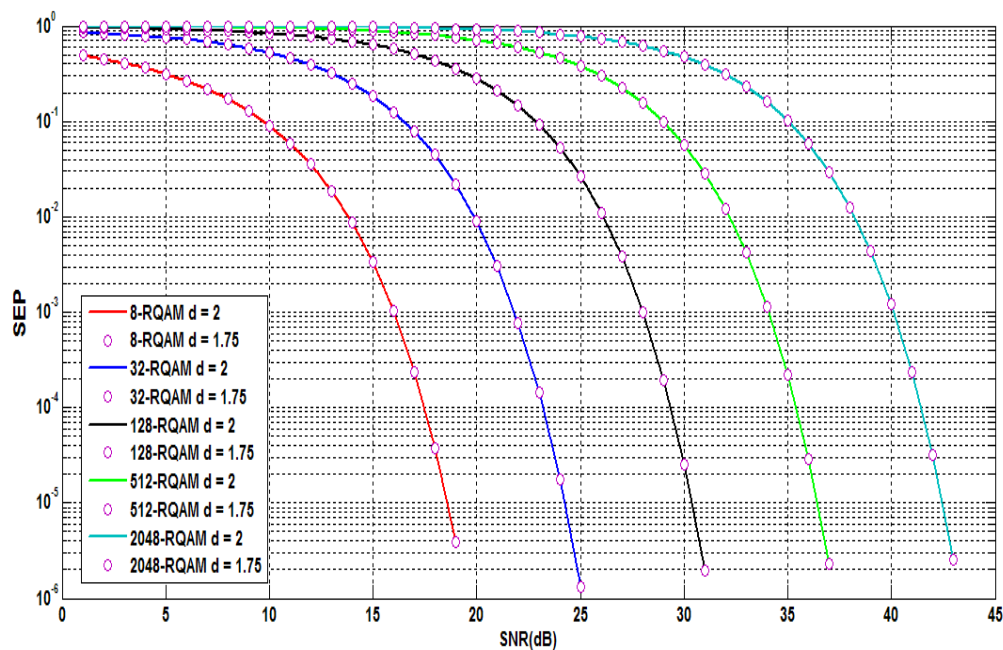


Fig.2.15 Symbol Error Probability of M-RQAM for Equal Energy over AWGN Channel

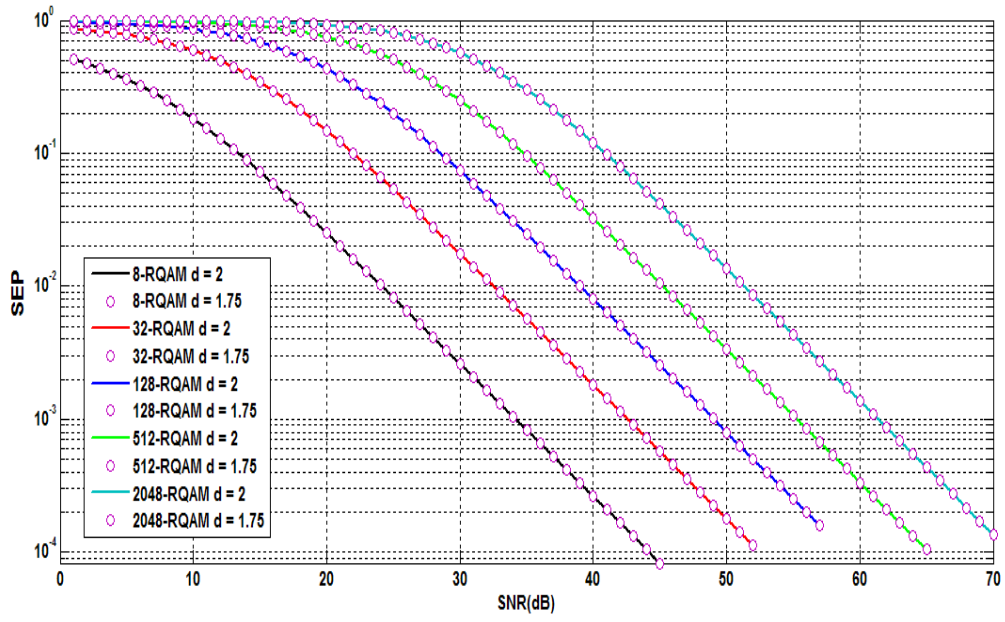


Fig.2.16 Symbol Error Probability of M-RQAM for Equal Energy over Rayleigh Channel

Chapter 3 BLIND EQUALIZATION

In communication, inter-symbol interference (ISI) is a form of distortion of a signal in which one symbol interferes with subsequent symbols. ISI degrades the communication system performance as the previous symbols have similar effect as noise, thus making the communication less reliable. ISI is caused by multipath propagation a channel causing successive symbols to "blur" together. Channel equalization is the process of reducing amplitude, frequency and phase distortion in a radio channel with the intent of improving transmission performance. In digital communication channel equalization is used to minimize the effect of ISI. We need to know channel statistics and initialize and adjust equalizer coefficients to set a channel. For unknown and time varying channels adaptive algorithms are used. For many applications a training sequence of known data is used to perform initialization as channel settings are determined on the basis of feedback of training sequence. Such equalization is called Training Equalization. A cost function is formed based on the output of the equalizer and statistical characteristics of the transmitted data and this cost unction is minimized with the help of stochastic gradient algorithm [15]. Disadvantage of this process is that sending sequence data occupies bandwidth and hence reduces channel capacity. Adaptive/Blind channel equalization without a training sequence is known as blind equalization. The major advantage of such a technique is that no training sequence is required to start or restart the system when the communication unexpectedly breaks down. The first blind equalization was presented in 1975 by Sato [16]. Since then large number of these blind equalization algorithms have proposed. Out of these, Multi Modulus Algorithm (MMA), Square Contour Algorithm (SCA), Generalized Cross Contour Algorithm (GCrCA) and Constant Modulus Algorithm (CMA) are notable.

3.1 System Model

The base band equivalent system model has been considered. The source at the transmitter generates independent and identically distributed (i.i.d) bits which are mapped to the constellation symbols. The symbols are inserted with noise and then passed through the channel to form the received signal. This received signal is then used as an input to the equalizer to obtain the channel taps.

3.2 Channel Model

The channel is like a linear time varying filter. The channel considered here is baseband equivalent [17] with complex impulse response. This impulse response is formulated as

$$h(\tau, t) = \sum_{k=1}^L \alpha_k(t) \delta(t - \tau_k(t)) \quad (3.1)$$

Where $\alpha_k(t)$ are the complex amplitudes and $\tau_k(t)$ are the multi paths. L is the total number of the multi paths of the channel. The channel impulse response is characterized by its [18] maximum excess delay i.e. τ_{\max} and coherence time. τ_{\max} determines the total number of taps of the sampled channel impulse response and the coherence bandwidth of the channel. The coherence bandwidth of the channel is the frequency range over which the frequency response of the channel is highly correlated. The more the τ_{\max} , lesser will be the coherence bandwidth and more distortion will the channel cause in the frequency spectrum of the transmitted signal. These multi paths as mentioned above introduce the ISI. The delayed impulses of the channel impulse response create multiple copies of the transmitted signal thus causing sum of the several delayed images of the transmitted signal to be received at the receiver. The mobility of the receiver or transmitter causes the values of $\alpha_k(t)$ to be changed with time. The counterpart of the coherence bandwidth is coherence time. It's the time for which the impulse response of the channel remains correlated. More the mobility of the user, lesser will be the coherence time. It is important to note that in small fading [5gul] the values of $\alpha_k(t)$ changes much faster than the position of the multi paths. Since blind equalization is used for static terminals, the channel impulse response remains constant over the time of

interest thus the coherence time of the channel is very large. If the channel is constant over the transmission time, the sampled channel impulse response h is given as

$$h(\tau, t) = \sum_{k=1}^L \alpha_k \delta(t - \tau_k) \quad (3.2)$$

Which in the vector notation can be written as $h = [h(0), h(1), \dots, h(L-1)]^T$. It is evident that static impulse response is the function of multi path only. Different channel models based on this model exist in literature e.g. voice Band Communication Channel [4gul], outdoor wireless channels “chan 1” – “chan 15 ” at <http://spib.rice.edu/spib/microwave.html>. The complex impulse response of voice band channel is shown in Fig 3.1

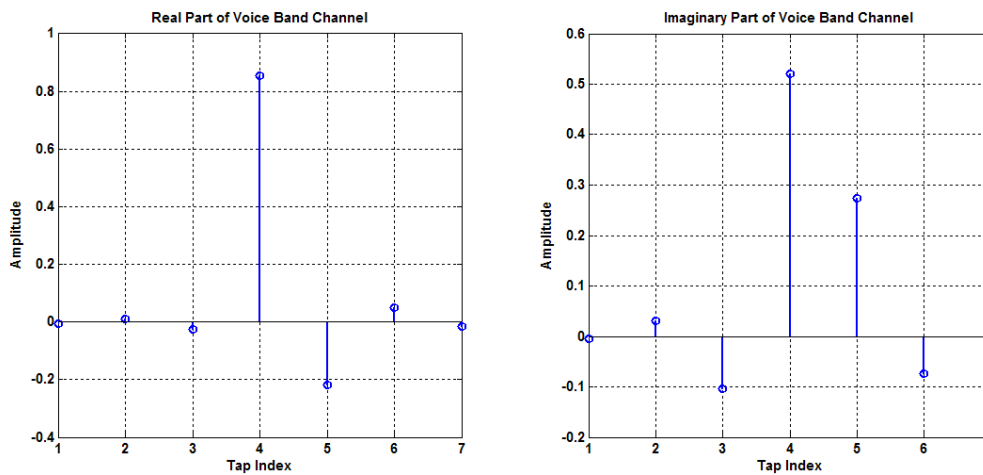


Fig.3.1 Impulse Response of the voice band channel

3.3 Equalizer model and Square contour Algorithm (SCA)

Consider the baseband representation for digital data transmission in Fig.3.2, where $s(n)$ are the independently identically distributed (i.i.d.) transmitted symbols, $v(n)$ is the additive white Gaussian noise (AWGN), $x(n)$ are the equalizer’s inputs and $a(n)$ are the estimated outputs at the decision device. The equalizer’s N -tap weight vector and input vector are defined as $W(n) = [w_0(n), w_1(n), \dots, w_{N-1}(n)]^T$ and $X(n) = [x(n), x(n-1), \dots, x(n-N+1)]^T$ respectively. We define $y(n) = W^T(n)X(n)$ as the equalizer output. The channel $h(n)$ is possibly a non minimum phase linear time invariant filter.

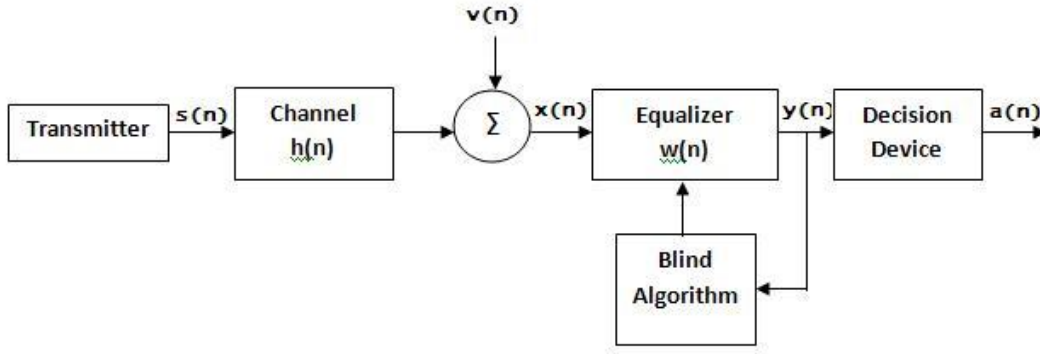


Fig. 3.2. Simplified baseband communication system

The objective is to achieve an estimate of $s(n)$ using $y(n)$ without using a training signal available at the receiver. To achieve the aforementioned objective, the SCA proposed by Thaiupathump and Kassam [19] combines the benefits of the well known reduced constellation algorithm (RCA) and the constant modulus algorithm (CMA). The SCA algorithm combines the reliable convergence benefit of CMA and the phase recovery feature of RCA. The generalized SCA cost function is:

$$J_{SCA} = E[(|y_R(n) + y_I(n)| + |y_R(n) - y_I(n)|)^p - (R_{SCA})^p]^2 \quad (3.3)$$

where $y_R(n)$ and $y_I(n)$ are the real and imaginary components of the equalizer $y(n)$. R_{SCA} is the constellation dependent dispersion constant, and p is the positive integer. The higher values of p enhance the algorithm at the cost of increased complexity. The corresponding tap update equation is obtained by differentiating the mean cost function in equ.3.3 with respect to equalizer tap weight w and then approximating the expectation with instantaneous values.

$$W(n+1) = W(n) - \mu e_{SCA}(n) X^*(n) \quad (3.4)$$

where $W(n+1)$ and $W(n)$ are the vectors comprising the next and current tap updates, respectively. $X(n)$ is the vector of equalizer input samples, $*$ denotes complex conjugate and $e_{SCA}(n)$ is the tap update error given by

$$e_{SCA} = (|y_R(n) + y_I(n)| + |y_R(n) - y_I(n)|)^p - (R_{SCA})^p \times \text{sgn}(|y_R(n) + y_I(n)| + |y_R(n) - y_I(n)|)^{p-1} \\ \times (\text{sgn}(y_R(n) + y_I(n))(1 + j) + \text{sgn}(y_R(n) - y_I(n))(1 - j)) \quad (3.5)$$

where sgn is the real signum function. For $p = 1$, the SCA error term in equ. (3.5) can be reiterated in the following form:

$$e_{SCA} = (|y_R(n) + y_I(n)| + |y_R(n) - y_I(n)| - R_{SCA})(\text{sgn}(y_R(n) + y_I(n))(1 + j) + \text{sgn}(y_R(n) - y_I(n))(1 - j)) \quad (3.6)$$

Dispersion constants in blind equalization algorithm play a critical part in adjusting the gain of the equalizer such that the statistics of the equalizer output is matched with the source constellation. The constant R_{SCA} is calculated by assuming the perfect equalization, i.e, $y(n) = s(n)$ and by setting the gradient $\nabla_w J_{SCA}$ to zero [19].

$$R_{SCA} = \frac{E[(|s_R(n) + s_I(n)| + |s_R(n) - s_I(n)|) R']}{E[R']} \quad (3.7)$$

$$\text{Where } R' = (|s_R(n) + s_I(n)| + |s_R(n) - s_I(n)|)(\text{sgn}(|s_R(n) + s_I(n)|) + \text{sgn}(|s_R(n) - s_I(n)|) + j(\text{sgn}(|s_R(n) + s_I(n)|) - \text{sgn}(|s_R(n) - s_I(n)|)))s^*(n) \quad (3.8)$$

where $s_R(n)$ and $s_I(n)$ are the real and imaginary components of source alphabet $s(n)$. At perfect equalization, SCA forces equalizer output to settle on a single on a single square contour of distance $R_{SCA} / 2$ (2.95, 6.38 and 12.98 for 16, 64 and 256-QAM, respectively) from the origin. The zero-error contour at distance 2.95 from the origin for 16-QAM is shown in Fig.3.3. It has been revealed through simulation results in [19] that for 16-QAM signal constellation, the performance of SCA is better than that of its parent algorithms i.e. RCA and CMA. Moreover, like MMA , SCA is capable of recovering and correcting the phase offset due to square modulus, but SCA is outperformed by MMA is terms of convergence speed and constellation eye opening. MMA is discussed in next section.

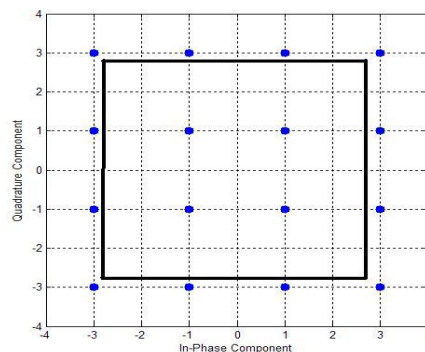


Fig. 3.3. Zero-error contour for SCA for 16-SQAM

3.4 Multi Modulus Algorithm (MMA)

The performance of RCA was improved by its generalization by Wesolowski [20], Oh et al [21] and Yang et al [22] and was termed as modified-CMA. The cost function of MCMA is given as

$$J_{MCMA} = \frac{1}{2p} E[(|y_R(n)|^p - R_R^p)^2 + (|y_I(n)|^p - R_I^p)^2] \quad (3.9)$$

A member of MCMA for $p = 2$ is popular as multi modulus algorithm (MMA) [20],[23]. The cost function of MMA is:

$$J_{MMA} = \frac{1}{4} E[(|y_R(n)|^2 - R_R^2)^2 + (|y_I(n)|^2 - R_I^2)^2] \quad (3.10)$$

The corresponding MMA weight tap updating equation is:

$$W(n+1) = W(n) - \mu[y_R(n)(y_R^2(n) - R_R^2) + jy_I(n)(y_I^2(n) - R_I^2)]x^*(n) \quad (3.11)$$

where $R_R^2 = \frac{E[s_R^4(n)]}{E[s_R^2(n)]}$ and $R_I^2 = \frac{E[s_I^4(n)]}{E[s_I^2(n)]}$ are dispersion constants. The corresponding zero-error points of MMA for 32-QAM is shown in Fig 3.4.

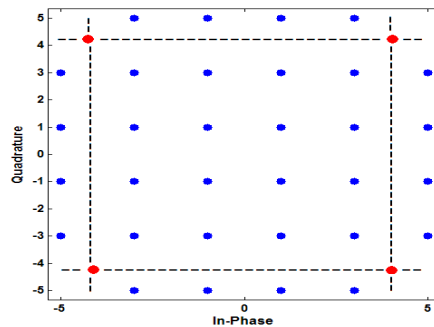


Fig.3.4 Zero-error Points for MMA for 32-QAM

The MMA algorithm is more suitable for square QAM. For cross QAM blind equalization algorithms have been obtained by tailoring RCA and MMA. In [23], [24] MMA is tailored to make it suitable for cross QAM as follows:

$$W(n+1) = W(n) - \mu[y_R(n)(y_R^2(n) - \tilde{R}_R^2) + jy_I(n)(y_I^2(n) - \tilde{R}_I^2)]x^*(n) \quad (3.12)$$

where

$$\tilde{R}_R^2 = \begin{cases} R_1^2, & |y_R(n)| \leq k \\ R_2^2, & |y_R(n)| > k \end{cases}, \text{ and, } \tilde{R}_I^2 = \begin{cases} R_1^2, & |y_I(n)| \leq k \\ R_2^2, & |y_I(n)| > k \end{cases} \quad (3.13)$$

The method for the evaluation of R_1^2 and R_2^2 is described in [23], [24]. In spite of its improved performance over equ.(3.11). There is problem associated with selecting the suitable value of threshold k in Eq.(A). The extensive simulation study shows that k value depends on size of cross QAM signal, ISI level of channel, phase-offset of channel and additive and convolutive noise. It is obvious that expect for the first factor remaining are not known a priori. Thus, it is not trivial to use cross QAM tailored MMA [21],[22]. The MMA when used for rectangular QAM however perform well [5] because it is less attracted to saddle points (thus increasing convergence speed) than the MMA that uses cross QAM because former has fewer saddle points than the latter.

3.5. Generalized Cross Contour Algorithm (GCrCA)

In this section we will be discussing another blind equalization algorithm tailored for cross QAM known as General Cross Contour Algorithm (GCrCA) Shafayat Abrar [6]. In the algorithm the author tailored the Generalized Square Contour Algorithm (GSCA) to have the cost function of GCrCA given as:

$$J_{GCrCA,k} = \frac{1}{2p} E[(|ky_R(n) + y_I(n)| + |ky_R(n) - y_I(n)| + |y_R(n) - ky_I(n)| + |y_R(n) + ky_I(n)| - |y_R(n) + y_I(n)| - |y_R(n) - y_I(n)|)^p - 2^p R^p]^2] \quad (3.14)$$

The corresponding tap weight update equation for this algorithm is obtained by differentiating the cost function (3.14) with respect to w and approximated the expectation with the instantaneous value. The equalizer tap weight vector is given as:

$$W(n+1) = W(n) - \mu\{(|A| + |B| + |C| + |D| - |E| - |F|)^p - 2^p R^p\} \cdot (|A| + |B| + |C| + |D| - |E| - |F|)^{p-1} \{k \operatorname{sgn}(A) + k \operatorname{sgn}(B) + \operatorname{sgn}(D) - \operatorname{sgn}(E) - \operatorname{sgn}(F) + j(\operatorname{sgn}(A) - \operatorname{sgn}(B) + k \operatorname{sgn}(C) - k \operatorname{sgn}(D) - \operatorname{sgn}(E) + \operatorname{sgn}(F))\} x^*(n) \quad (3.15)$$

where $A = \{ky_R(n) + y_I(n)\}$, $B = \{ky_R(n) - y_I(n)\}$, $C = \{y_R(n) + ky_I(n)\}$, $D = \{y_R(n) - ky_I(n)\}$,

$E = \{y_R(n) + y_I(n)\}$, and, $F = \{y_R(n) - y_I(n)\}$, R_{Cr}^p and k are constellation dependent parameter given as

$$R_{Cr}^p = \frac{1}{2^p} \frac{E[(|\bar{A}| + |\bar{B}| + |\bar{C}| + |\bar{D}| - |\bar{E}| - |\bar{F}|)^{2p}]}{E[(|\bar{A}| + |\bar{B}| + |\bar{C}| + |\bar{D}| - |\bar{E}| - |\bar{F}|)^p]} \quad (3.16)$$

where $\bar{A} = \{ks_R(n) + s_I(n)\}$, $\bar{B} = \{ks_R(n) - s_I(n)\}$, $\bar{C} = \{s_R(n) + ks_I(n)\}$, $\bar{D} = \{s_R(n) - ks_I(n)\}$,

$\bar{E} = \{s_R(n) + s_I(n)\}$, and, $\bar{F} = \{s_R(n) - s_I(n)\}$ and for $p=2$ the value of k , k_{opt} is given as

$$k_{opt} = \arg \min_k \left\{ \frac{G_1 E[a_R^6] - G_2 R^2 E[a_R^4] + G_3 R^4 E[a_R^2]}{G_4 E[a_R^2] - R^2} \right\} \quad (3.17)$$

where $G_1 = 4(k^7 - k + 1)$, $G_2 = 8(k^5 - k + 1)$, $G_3 = 4(k^3 - k + 1)$ and $G_4 = 3(k^3 - k + 1)$.

In spite of its improved performance over its parent algorithm, the GCrCA work only with Cross QAM and is not flexible for square QAM thus hindering the ease of implementation, secondly the value of k_{opt} is difficult to obtain as there is no close form equation to do so. The equ.(3.17) for k_{opt} needs to minimize the arguments on all possible values of k i.

Thus a new blind equalization algorithm is required which will provide ease of implementation for both non square (rectangular) QAM for odd bits and Square QAM for even bits. In next chapter Rectangular Contour Algorithm is proposed in this regard. The simulation results in chapter 4 confirm that the proposed algorithm outperform the above mentioned algorithms in term of mean square error (MSE) and residual ISI.

Chapter 4 RECTANGULAR CONTOUR ALGORITHM

The main advantage of using Rectangular QAM is that it is better able to recover the phase rotation introduced by channels than can Square and Cross QAM constellations, accordingly any phase error within 180° can be correctly detected thus giving advantage in blind equalization [5]. Secondly the implementation and calculation of the average symbol error probability (SEP) of Cross QAM are more complicated compared to that of Square and Rectangular QAMs since the inphase and quadrature components of Cross-QAMs cannot be demodulated independently. So, the calculation of SEP of Cross QAM cannot be reduced to a one dimensional problem by using independence of the inphase and quadrature components as can be done for Square and Cross QAMs [25]. Third the Gray Coding can be done more easily when using Rectangular QAM than the Cross QAM of same order which can provide an ease in improving the performance of Personal Area Network (PAN) systems [26] where this gray coding is required for QAM with odd bits. The reason that the Rectangular QAM is being neglected so far is because it requires more energy to transmit symbols however this problem can be overcome by reducing distance between two adjacent points in the rectangular constellation to 1.75 instead of 2 so that the average transmitted power for both cross and rectangular become almost identical and its SEP remains same as shown in chapter 2. It is also shown in section 4.3 that even with equal transmitted power blind equalizers using Rectangular constellation outperforms the equalizers using cross QAM in terms of MSE and ISI.

4.1 Rectangular Contour Algorithm ($R_{RECT}CA$)

The SCA discussed in chapter 3 can be modified to achieve better results by further reducing the mismatch between the cost function and the transmitted constellation consequently accomplishing fast convergence rate for Rectangular QAM for odd k. From the most popular constant modulus algorithm (CMA) we have

$$J_{CMA} = E[|y_R(n)|^2 - R_{CMA}^2]^2 \quad (4.1)$$

And its zero-error contour is shown in Fig.4.1. It is clear that minimizing the CMA cost function in equ.(4.1) is equivalent to minimize the dispersion of the equalizer output around

circle of radius R_{CMA} similarly minimizing SCA cost function in equation (3.3) of chapter 3 is equivalent to minimize the dispersion of the equalizer output around square of side $R_{SCA} / 2$

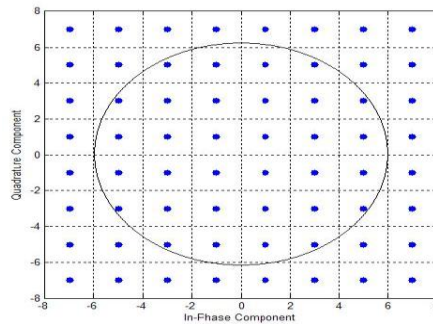


Fig.4.1. Zero-error contour for CMA for 64-SQAM

For a circle of radius R_{CMA} , we have the relationship as

$$|y(n)| = R_{CMA} \quad (4.2)$$

For square we have the relationship

$$\max[|y_R(n)|, |y_I(n)|] = R' \quad (4.3)$$

which may be rewritten as

$$\begin{aligned} \max[|y_R(n)|, |y_I(n)|] &= |y_R(n) + y_I(n)| + |y_R(n) - y_I(n)| / 2 \\ &= |y_R(n) + y_I(n)| + |y_R(n) + y_I(n)| / 2 = R' \end{aligned} \quad (4.4)$$

For simplicity of notation, let $R_{SCA} = 2R'$

$$\max[|y_R(n)|, |y_I(n)|] = |y_R(n) + y_I(n)| + |y_R(n) + y_I(n)| = R_{SCA} \quad (4.5)$$

For rectangle, we have the relationship

$$\max \left[\frac{|y_R(n)|}{|a|}, \frac{|y_I(n)|}{|b|} \right] = R \quad (4.6)$$

which may be rewritten as

$$\begin{aligned} \max \left[\frac{|y_R(n)|}{|a|}, \frac{|y_I(n)|}{|b|} \right] &= \frac{\left| \frac{y_R(n)}{a} + \frac{y_I(n)}{b} \right| + \left| \frac{y_R(n)}{a} - \frac{y_I(n)}{b} \right|}{2} \\ &= \frac{|by_R(n) + ay_I(n)| + |by_R(n) - ay_I(n)|}{2|ab|} = R \end{aligned} \quad (4.7)$$

For simplicity of notation, let $R_{RECT} = 2R$ then

$$\max \left[\frac{|y_R(n)|}{|a|}, \frac{|y_I(n)|}{|b|} \right] = |by_R(n) + ay_I(n)| + |by_R(n) - ay_I(n)| = |ab| R_{RECT} \quad (4.8)$$

We then obtain the cost function of the rectangular contour algorithm as

$$J_{RECT} = E[(|by_R(n) + ay_I(n)| + |by_R(n) - ay_I(n)| - |ab| R_{RECT})^2] \quad (4.9)$$

with R_{RECT} a positive real constant which will be discussed shortly in the section, with a and b also are Rectangular QAM constellation dependent parameters defining spread along in-phase and quadrature axis e.g. for 32-QAM in Fig.4.2 $a = 7$ and $b = 3$. The zero-error contour of the rectangular contour algorithm is shown in Fig.4.2. Since the cost function employs both modulus and phase of the equalizer output, carrier phase recovery can also be accomplished along with the blind equalization process.

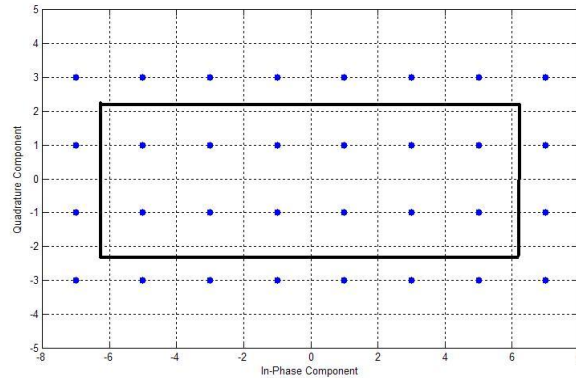


Fig.4.2. Zero-error contour for $R_{RECT}CA$ with $a = 7$, $b = 3$ for 32-RQAM

To obtain the tap update equation for the proposed algorithm, we differentiate the mean cost function in equ. (4.9) with respect to equalizer tap weight w .

$$\begin{aligned}
\nabla_w \mathbf{J}_{RECT} &= E[(|by_R(n) + ay_I(n)| + |by_R(n) - ay_I(n)| - |ab| R_{RECT}) \\
&\quad \cdot \{b \operatorname{sgn}[by_R(n) + ay_I(n)] + b \operatorname{sgn}[by_R(n) - ay_I(n)] \\
&\quad + j(a \operatorname{sgn}[by_R(n) + ay_I(n)] - a \operatorname{sgn}[by_R(n) - ay_I(n)])\} x^*(n)] \quad (4.10)
\end{aligned}$$

Approximating the expectation with the instantaneous value yields

$$\begin{aligned}
\nabla_w \mathbf{J}_{RECT} &= (|by_R(n) + ay_I(n)| + |by_R(n) - ay_I(n)| - |ab| R_{RECT}) \\
&\quad \cdot \{b \operatorname{sgn}[by_R(n) + ay_I(n)] + b \operatorname{sgn}[ay_R(n) - ay_I(n)] \\
&\quad + j(a \operatorname{sgn}[by_R(n) + ay_I(n)] - a \operatorname{sgn}[by_R(n) - ay_I(n)])\} x^*(n) \quad (4.11)
\end{aligned}$$

The equalizer tap weight vector is adapted according to

$$\begin{aligned}
w(n+1) &= w(n) - \mu \{ (|by_R(n) + ay_I(n)| + |by_R(n) - ay_I(n)| - |ab| R_{RECT}) \\
&\quad \cdot (b \operatorname{sgn}[by_R(n) + ay_I(n)] + b \operatorname{sgn}[by_R(n) - ay_I(n)] \\
&\quad + j(a \operatorname{sgn}[by_R(n) + ay_I(n)] - a \operatorname{sgn}[by_R(n) - ay_I(n)]))\} x^*(n) \quad (4.12)
\end{aligned}$$

The constant R_{RECT} can now be evaluated by assuming perfect equalization, i.e. $y(n) = s(n)$ and by setting the gradient $\nabla_w \mathbf{J}_{RECT}$ to zero

$$\begin{aligned}
&E[(|bs_R(n) + as_I(n)| + |bs_R(n) - as_I(n)| - |ab| R_{RECT}) \\
&\quad \cdot \{b \operatorname{sgn}[bs_R(n) + as_I(n)] + b \operatorname{sgn}[bs_R(n) - as_I(n)] \\
&\quad + j(a \operatorname{sgn}[bs_R(n) + as_I(n)] - a \operatorname{sgn}[bs_R(n) - as_I(n)])\} x^*(n)] = 0 \quad (4.13)
\end{aligned}$$

Solving for R_{RECT} we have

$$R_{RECT} = \frac{E[(|bs_R(n) + as_I(n)| + |bs_R(n) - as_I(n)|) \cdot R^o]}{|ab| E[R^o]} \quad (4.14)$$

where

$$\begin{aligned}
R^o &= \{b \operatorname{sgn}[bs_r(n) + as_l(n)] + b \operatorname{sgn}[bs_r(n) - as_l(n)] \\
&+ j(a \operatorname{sgn}[bs_r(n) + as_l(n)] - a \operatorname{sgn}[bs_r(n) - as_l(n)])\} \cdot s^*(n)
\end{aligned} \tag{4.15}$$

It should be worth noting that just putting $a = 1$ and $b = 1$ the $R_{\text{RECT}}\text{CA}$ reduces to SCA thus providing ease of implementation for both odd and even bits QAM signals.

4.2 Generalized Rectangular Contour Algorithm ($GR_{\text{RECT}}\text{CA}$)

The section provides a family of blind equalization algorithms that has a rectangular zero-error contour. The Rectangular Contour Algorithm introduced in the previous section is generalized by using additional parameter p in the same way as defined for the Square contour algorithm family in [5]. The mean cost function of the generalized Rectangular Contour Algorithm is given by

$$J_{\text{GRECT}} = E[(|by_r(n) + ay_l(n)| + |by_r(n) - ay_l(n)|)^p - (|ab| R_{\text{GRECT}})^p]^2 \tag{4.16}$$

where p is a positive integer. In practice, p will generally be limited to 1 and 2, thus for $p = 1$ we obtain cost function of $R_{\text{RECT}}\text{CA}$ defined in equ (4.9) and for $p = 2$ it is given by

$$J_{\text{GRECT}, p=2} = E[(|by_r(n) + ay_l(n)| + |by_r(n) - ay_l(n)|)^2 - (|ab| R_{\text{GRECT}})^2]^2 \tag{4.17}$$

To obtain the update equation for the Generalized Rectangular Contour Algorithm, differentiate the cost function in equ (4.16) with respect to w and approximate the expectation with the instantaneous values yields

$$\begin{aligned}
\nabla_w J_{\text{GRECT}} &= ((|by_r(n) + ay_l(n)| + |by_r(n) - ay_l(n)|)^p - (|ab| R_{\text{GRECT}})^p) \\
&\quad (|by_r(n) + ay_l(n)| + |by_r(n) - ay_l(n)|)^{p-1} \\
&\quad \cdot \{b \operatorname{sgn}[by_r(n) + ay_l(n)] + b \operatorname{sgn}[ay_r(n) - ay_l(n)] \\
&\quad + j(a \operatorname{sgn}[by_r(n) + ay_l(n)] - a \operatorname{sgn}[ay_r(n) - ay_l(n)])\} \cdot x^*(n)
\end{aligned} \tag{4.18}$$

The constant R_{GRECT}^p can be evaluated by assuming perfect equalization, i.e. $y(n) = s(n)$ and setting the gradient $\nabla_w J_{\text{GRECT}}$ to zero. Then, solving for R_{GRECT}^p

$$R_{\text{GRECT}}^p = \frac{E[(|bs_r(n) + as_l(n)| + |bs_r(n) - as_l(n)|)^p \cdot R^n]}{|ab|^p E[R^n]} \tag{4.19}$$

where

$$R'' = (|bs_R(n) + as_I(n)| + |bs_R(n) - as_I(n)|)^{p-1} \cdot \{b \operatorname{sgn}[bs_R(n) + as_I(n)] + b \operatorname{sgn}[bs_R(n) - as_I(n)] + j(a \operatorname{sgn}[bs_R(n) + as_I(n)] - a \operatorname{sgn}[bs_R(n) - as_I(n)])\} \cdot s^*(n) \quad (4.20)$$

Table 1 shows values of constants R_{GRECT} of $\text{GR}_{\text{RECT}}\text{CA}$ ($p = 1, 2$) along with parameter a and b for Rectangular QAM.

	8RQAM (4x2)	32RQAM (8x4)	128RQAM (16x8)
$R_{\text{GRECT}} (p=1)$	2	1.7927	1.6445
$R_{\text{GRECT}} (p=2)$	2	1.9122	1.7827
a	3	7	15
b	1	3	7

Table 4.1 Values of R_{GRECT} of $\text{GR}_{\text{RECT}}\text{CA}$ ($p = 1, 2$) & parameter a and b

4.3 Steady-state error analysis for the Rectangular Contour Algorithm

Now we will be studying the steady-state MSE performance of Rectangular contour algorithm in the noise free case by following the approach proposed in [27]-[28]. For an adaptive algorithm of the form

$$w(n+1) = w(n) - \mu e_{\text{RECT}}(n) x^*(n) \quad (4.21)$$

Let $\Delta w(n)$ be the difference between the current equalizer $w(n)$ and the optimum equalizer weight w_{opt} . The condition

$$E\{\|\Delta w(n+1)\|^2\} = E\{\|\Delta w(n)\|^2\} \quad (4.22)$$

Holds in steady state ($n \rightarrow \infty$). By defining a priori estimation error $e_a(n) = \Delta w^T(n)x(n)$, for the adaptive algorithm, we have in general

$$E \left\{ \frac{|e_a(n)|^2}{\|x(n)\|^2} \right\} = E \left\{ \frac{1}{\|x(n)\|^2} |e_a(n) - \mu \|x(n)\|^2 e(n)| \right\} \quad (4.23)$$

For simplification in the calculations we drop the time index n thus equ (4.23) becomes

$$E \left\{ \frac{|e_a|^2}{\|x\|^2} \right\} = E \left\{ \frac{|e_a|^2}{\|x\|^2} \right\} - \mu E \{ e_a^* e + e_a e^* \} + \mu^2 E \{ \|x\|^2 |e|^2 \} \quad (4.24)$$

We assume that

$$\begin{aligned} Q_1 &= \mu E \{ e_a^* e + e_a e^* \}, \\ Q_2 &= \mu^2 E \{ \|x\|^2 |e|^2 \}. \end{aligned}$$

Putting values of Q_1 and Q_2 the equ (4.24) becomes

$$E \left\{ \frac{|e_a|^2}{\|x\|^2} \right\} = E \left\{ \frac{|e_a|^2}{\|x\|^2} \right\} - Q_1 + Q_2 \quad (4.25)$$

Clearly the terms Q_1 and Q_2 are identical, so an appropriate expression for steady-state MSE $E \{ |e_a|^2 \}$. following are the assumptions [27] made in the analysis of the steady-state MSE for R_{RECT}CA:

- The step size parameter μ is sufficiently small and the value of $|e_a|^2$ is reasonably low at steady-state
- The transmitted symbols $s(n)$ and the estimated error $e_a(n)$ are independent in the steady-state and $E \{ s(n)e_a(n) \} = 0$ since $s(n)$ has zero mean.
- The scaled regressor energy is independent of $y(n)$ and $e_a(n)$ in steady state.

The error function of R_{RECT}CA with elimination of time index is given as:

$$e_{RECT} = 4by_R \left(4b^2 y_R^2 - (|ab| 2R_{RECT})^2 \right) A + j4ay_I \left(4a^2 y_I^2 - (|ab| 2R_{RECT})^2 \right) B. \quad (4.26)$$

$$\begin{aligned} \text{Where} \quad A &= \frac{\text{sgn}(by_R)}{2} \left(\text{sgn}(by_R + ay_I) + \text{sgn}(by_R - ay_I) \right). \\ B &= \frac{\text{sgn}(ay_I)}{2} \left(\text{sgn}(by_R + ay_I) - \text{sgn}(by_R - ay_I) \right). \end{aligned}$$

After some simplification and replacing R_{RECT}^2 with R we have:

$$e_{RECT} = 16by_R \left(b^2 y_R^2 - |ab|^2 R \right) A + j16ay_I \left(a^2 y_I^2 - |ab|^2 R \right) B. \quad (4.27)$$

where a and b are constellation dependent parameters. We can replace y by $s + e_a$, where s is transmitted symbol and e_a is a priori estimation error. Similarly the real and imaginary components of equalizer outputs y_R can be replaced with $s_R + e_{aR}$ and y_I with $s_I + e_{aI}$.

Consequently, for $e = e_R + je_I$ thus equ (4.22) can be decomposed as

$$\begin{aligned} e_R &= 16b(s_R + e_{aR})(b^2(s_R + e_{aR})^2 - |ab|^2 R)A. \\ e_I &= 16a(s_I + e_{aI})(a^2(s_I + e_{aI})^2 - |ab|^2 R)B. \end{aligned}$$

Computing Q_1 , we obtain

$$\begin{aligned} Q_1 &= 32\mu E \left\{ \left(e_{aR}(b^3 s_R^3 - b s_R |ab|^2 R) + e_{aR}^2(3b^3 s_R^2 - b |ab|^2 R) + 3b^3 s_R e_{aR}^3 + b^3 e_{aR}^4 \right) A \right\} \\ &\dots\dots + 32\mu E \left\{ \left(e_{aI}(a^3 s_I^3 - a s_I |ab|^2 R) + e_{aI}^2(3a^3 s_I^2 - a |ab|^2 R) + 3a^3 s_I e_{aI}^3 + a^3 e_{aI}^4 \right) B \right\}. \end{aligned} \quad (4.28)$$

Using the assumed independence of s and e_a and neglecting $2\mu b^3 E\{e_{aR}^4\}$ and $2\mu a^3 E\{e_{aI}^4\}$ for small μ and small e_{aR}^2 and e_{aI}^2 we obtain the approximation

$$Q_1 \approx 2\mu E \left\{ 16e_{aR}^2(3b^3 s_R^2 - b |ab|^2 R)A + 16e_{aI}^2(3a^3 s_I^2 - a |ab|^2 R)B \right\} \quad (4.29)$$

Letting $E\{e_{aR}^2\} = E\{e_{aI}^2\}$, equ (4.29) can be written as

$$Q_1 \approx 2\mu E \left\{ 16(3b^3 s_R^2 - b |ab|^2 R)A + 16(3a^3 s_I^2 - a |ab|^2 R)B \right\} E\{e_{aR}^2\} \quad (4.30)$$

Now for obtaining Q_2 we assumed that the statistics of s_R and s_I are the same. Using the assumed independence of $\mu^2 \|x\|^2$ and $y(n)$ and ignoring the terms with $E\{e_{aR}^4\}$, $E\{e_{aI}^4\}$, $E\{e_{aR}^6\}$ and $E\{e_{aI}^6\}$, the value of Q_2 can be computed as

$$\begin{aligned}
Q_2 \approx & 256\mu^2 E \left\{ \left(b^6 s_R^6 - 2b^4 |ab|^2 R s_R^4 + b^2 |ab|^4 R^2 s_R^2 \right) A + \left(a^6 s_I^6 - 2a^4 |ab|^2 R s_I^4 + a^2 |ab|^4 R^2 s_I^2 \right) B \right\} E \left\{ \|x\|^2 \right\} \\
& + 256\mu^2 E \left\{ e_{aR}^2 \left(15b^6 s_R^4 - 12b^4 |ab|^2 R s_R^2 + b^2 |ab|^4 R^2 \right) \right\} E \left\{ \|x\|^2 \right\} \\
& + 256\mu^2 E \left\{ e_{aI}^2 \left(15a^6 s_I^4 - 12a^4 |ab|^2 R s_I^2 + a^2 |ab|^4 R^2 \right) \right\} E \left\{ \|x\|^2 \right\} \quad (4.31)
\end{aligned}$$

Letting $E \left\{ e_{aR}^2 \right\} = E \left\{ e_{aI}^2 \right\}$, we get further approximation of equ.(4.31)

$$\begin{aligned}
Q_2 \approx & 256\mu^2 E \left\{ \left(b^6 s_R^6 - 2b^4 |ab|^2 R s_R^4 + b^2 |ab|^4 R^2 s_R^2 \right) A + \left(a^6 s_I^6 - 2a^4 |ab|^2 R s_I^4 + a^2 |ab|^4 R^2 s_I^2 \right) B \right\} E \left\{ \|x\|^2 \right\} \\
& + 256\mu^2 E \left\{ \left(15b^6 s_R^4 - 12b^4 |ab|^2 R s_R^2 + b^2 |ab|^4 R^2 \right) + \left(15a^6 s_I^4 - 12a^4 |ab|^2 R s_I^2 + a^2 |ab|^4 R^2 \right) \right\} E \left\{ e_{aR}^2 \right\} E \left\{ \|x\|^2 \right\} \quad (4.32)
\end{aligned}$$

since $Q_1 = Q_2$ and $R = R_{RECT}$ the steady state MSE for the Rectangular Contour Algorithm can be approximated as

$$\begin{aligned}
E \left\{ |e_a|_{RECT}^2 \right\} \approx & \frac{256E \left\{ \left(b^6 s_R^6 - 2b^4 |ab|^2 R s_R^4 + b^2 |ab|^4 R^2 s_R^2 \right) A + \left(a^6 s_I^6 - 2a^4 |ab|^2 R s_I^4 + a^2 |ab|^4 R^2 s_I^2 \right) B \right\}}{E \left\{ 16(3b^3 s_R^2 - b |ab|^2 R) A + 16(3a^3 s_I^2 - a |ab|^2 R) B \right\} / \mu E \left\{ \|x\|^2 \right\} - 128E \left\{ \left(15b^6 s_R^4 - 12b^4 |ab|^2 R s_R^2 + b^2 |ab|^4 R^2 \right) + \left(15a^6 s_I^4 - 12a^4 |ab|^2 R s_I^2 + a^2 |ab|^4 R^2 \right) \right\}} \quad (4.33)
\end{aligned}$$

Fig.4.3 shows the Steady State MSE and simulation for different values of μ .

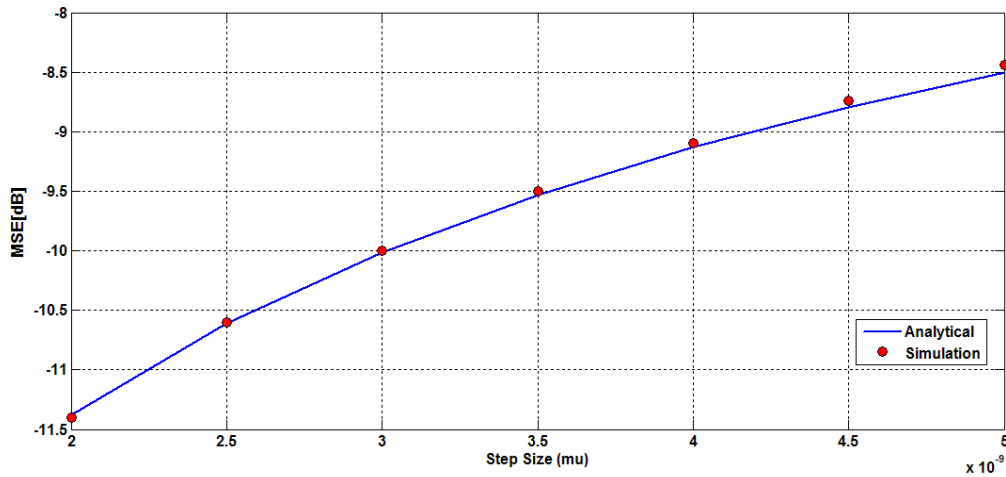


Fig.4.3 Steady-State Mean Square Error of $R_{RECT}CA$

4.4 Simulation Results and Discussions

The computer simulation is provided in this section. We use the 32-RQAM and 128-RQAM signal constellations with a minimum distance between symbols of 2 and then to have equal transmitted power as 32-XQAM and 128-XQAM, we use 32-RQAM and 128-RQAM with minimum distance between symbols of 1.75 thus giving 19.9 and 81.66 of energies respectively which are almost identical to energies of 32-XQAM and 128-XQAM, 20 and 82 respectively. A 7-tap equalizer is initialized with value 1 for the centre tap, the other being zero. A typical voice-band communication channel is used. Fig 4.4 represents the steady state performance of $R_{RECT}CA$, SCA, MMA and GCrCA for 32-QAM signal constellation. For fair comparison GCrCA, SCA and MMA are simulated with 32-XQAM while $R_{RECT}CA$ with 32-RQAM. MMA is also simulated with 32-RQAM for the improved performance over MMA using 32-XQAM. The noise power is adjusted such that it gives rise to a channel signal-to-noise ratio (SNR) of 30dB. The adaptive gain for $R_{RECT}CA$ is taken as $\mu_{RECT} = 2.5e-9$, for MMA with 32-RQAM $\mu_{MMARQAM} = 2e-6$, for GCrCA it is taken to be $\mu_{GCrCA} = 3.4e-6$, for MMA with 32-XQAM, $\mu_{MMAXQAM} = 6e-6$ to achieve the same MSE floor level of approximately -10dB. However the SCA is not able to achieve the same error floor in current environment thus for SCA $\mu_{SCA} = 0.4e-6$ so that it can be as much close to error floor of -10dB as possible. It is evident from the Fig 4.4 that the $R_{RECT}CA$ is achieving faster convergence than those of MMA with 32-XQAM and 32-RQAM, GCrCA and SCA for same steady-state performance. The experimental values are generated as an average over 40 trials.

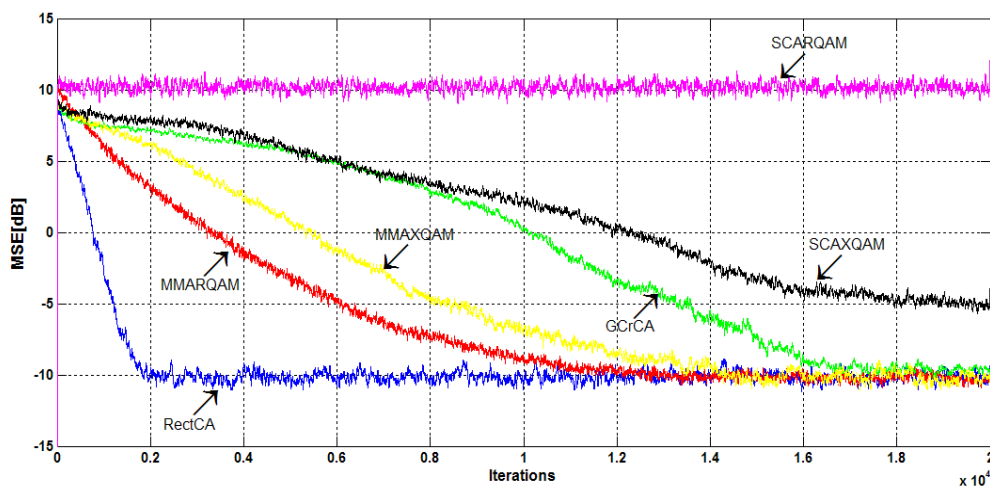


Fig.4.4 MSE traces for 32-XQAM and 32-RQAM (2 distance b/w symbols)

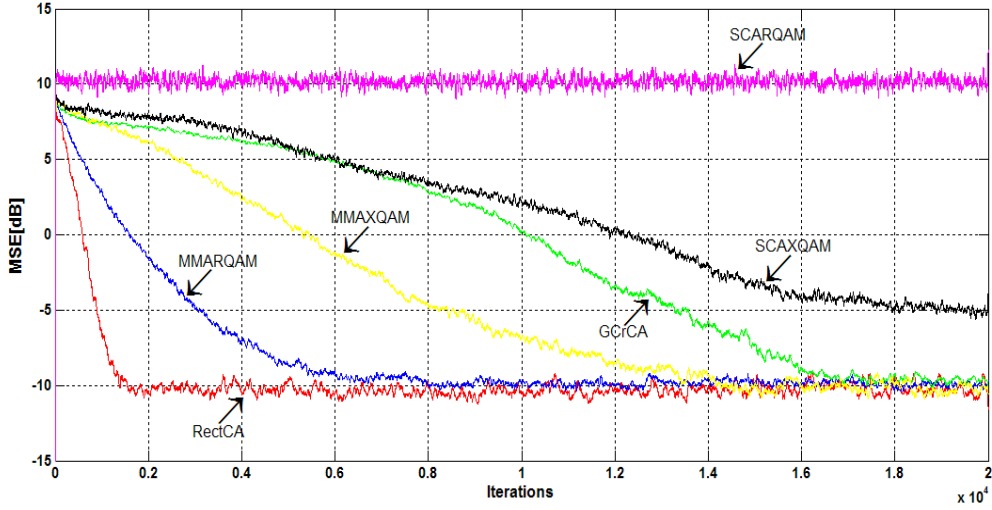


Fig.4.5 MSE traces for 32-XQAM and 32-RQAM (1.75 distance b/w symbols)

Fig 4.5 shows the steady-state performance of above mentioned blind equalization algorithms under the same environment as mentioned above but with 32-RQAM having minimum distance of 1.75 between adjacent symbols to have equal energy as 32-XQAM. Again we use 32-XQAM with minimum distance of 2 between symbols for GCrCA, SCA and MMA while 32-RQAM with 1.75 as distance for MMA and R_{RECTCA} . The adaptive gain for R_{RECTCA} is taken as $\mu_{RECT} = 10e-9$, for MMA with 32-RQAM $\mu_{MMARQAM} = 6e-6$ and MMA with 32-XQAM $\mu_{MMAXQAM} = 6e-6$ while for GCrCA it is taken to be $\mu_{GCrCA} = 3e-6$ to achieve the same MSE floor level of approximately -10dB. $\mu_{SCA} = 0.4e-6$ again for the above stated reason for SCA. It is again evident from Fig 4.5 that R_{RECTCA} outperforms MMA (32-RQAM & 32-XQAM), SCA and GCrCA in terms of convergence while keeping the MSE floor same as approximately -10dB.

The performance of GCrCA and MMA with 32-XQAM and MMA, R_{RECTCA} with 32-R QAM with minimum distance between symbols of 2 and 1.75 in Fig 4.6 and Fig 4.7 respectively in terms of suppression of residual inter symbol interference ISI is evaluated in computer simulations. SCA is not considered because of its undesirable performance in the current environment. The residual ISI at the output of the equalizer and SNR at the input of the equalizer are calculated by Eqs. (38) and (39) in [14]. The noise power is adjusted such that it gives rise to a channel signal-to-noise ratio (SNR) of 30dB. The adaptive gain for R_{RECTCA} is taken as $\mu_{RECT} = 0.5e-9$, for MMA with RQAM $\mu_{MMARQAM} = 2e-6$, for GCrCA it is taken to be

$\mu_{\text{GCrCA}} = 3\text{e-}6$ and for MMA with XQAM $\mu_{\text{MMA XQAM}} = 5\text{e-}6$ so that all the equalizers get approximately same convergence rate. Fig 4.6 depicts the residual ISI traces for all the schemes in which the superior behavior of R_{RECTCA} blind equalizer is evident. Fig 4.7 shows the same residual ISI plot but for 32-RQAM with minimum of 1.75 distance between symbols for MMA and R_{RECTCA} and 32-XQAM for GCrCA and MMA with adaptive gain for R_{RECTCA} is taken as $\mu_{\text{RECT}} = 2\text{e-}9$, for MMA with RQAM $\mu_{\text{MMA RQAM}} = 4\text{e-}6$, for GCrCA it is taken to be $\mu_{\text{GCrCA}} = 3\text{e-}6$ and for MMA with XQAM $\mu_{\text{MMA XQAM}} = 5\text{e-}6$. Again it is evident that R_{RECTCA} outperforms other blind equalizers.

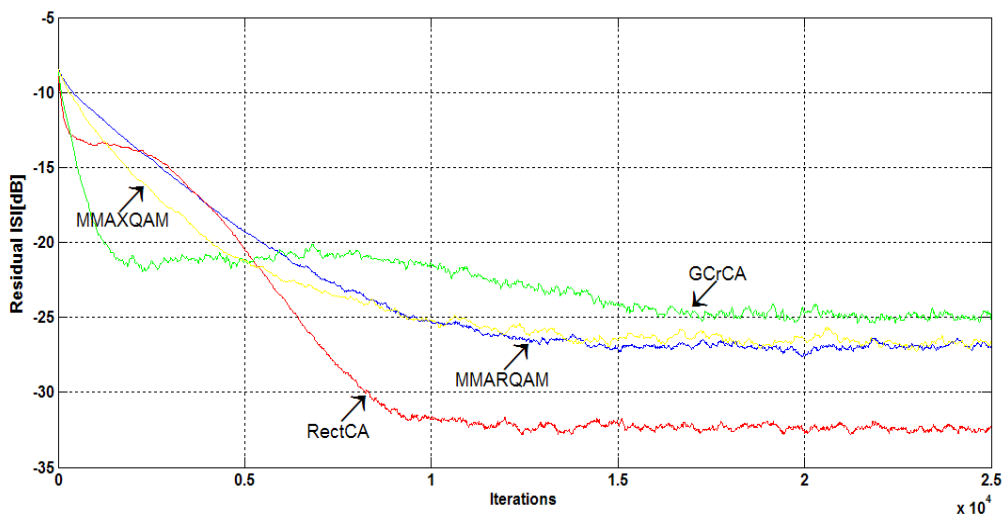


Fig.4.6 Residual ISI traces for 32-XQAM and 32-RQAM (2 distance b/w symbols)

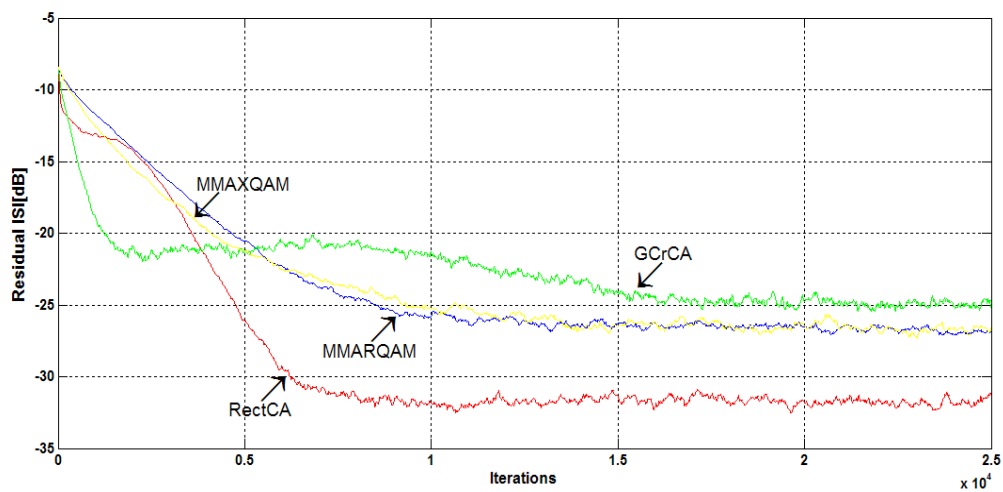


Fig.4.7 Residual ISI traces for 32-XQAM and 32-RQAM (1.75 distance b/w symbols)

Now we compare the performance of the MMA, $R_{RECT}CA$, SCA and GCrCA blind equalizers using 128-QAM using voice band communication channel. Fig 4.8 and Fig 4.9 show the steady-state performance of $R_{RECT}CA$, MMA, GCrCA and SCA. We use 128-XQAM for GCrCA, SCA and MMA in both figures while 128-RQAM with minimum distance of 2 between symbols in Fig 4.8 and 128-RQAM with minimum distance of 1.75 in Fig 4.9 for MMA and $R_{RECT}CA$. The noise power is adjusted such that it gives rise to a channel signal-to-noise ratio (SNR) of 30dB. The adaptive gain for $R_{RECT}CA$ is taken as $\mu_{RECT}= 1.5e-12$, for MMA with RQAM $\mu_{MMARQAM}= 6e-8$, for GCrCA $\mu_{GCrCA}= 7e-8$, for SCA $\mu_{SCA}= 1e-8$ and for MMA with XQAM $\mu_{MMARQAM}= 2e-7$ to achieve the same MSE floor level of approximately -5dB in Fig 4.8 while $\mu_{RECT}= 4e-12$, $\mu_{MMAQAM}= 10e-8$, $\mu_{GCrCA}= 4e-8$, $\mu_{SCA}= 1e-8$ and $\mu_{MMAQAM}= 1e-7$ in Fig 4.9 to have MSE floor level of approximately -6 dB . In Fig 4.8 and Fig 4.9 it is quite evident that the $R_{RECT}CA$ outperforms the MMA (with 128RQAM & 128XQAM) , GCrCA and SCA in term of convergence rate. The experimental values are generated as an average over 40 trials.

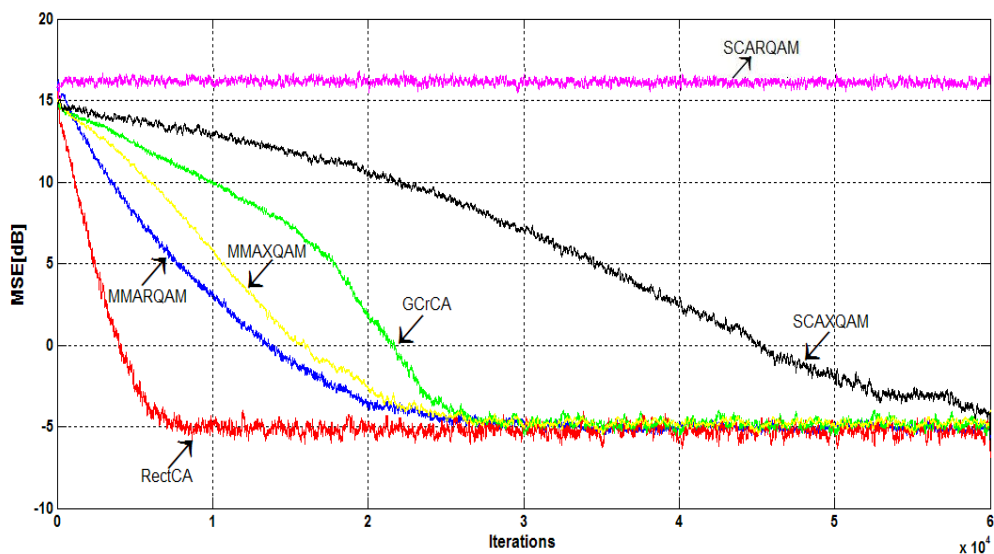


Fig.4.8 MSE traces for 128-XQAM and 128-RQAM (2 distance b/w symbols)

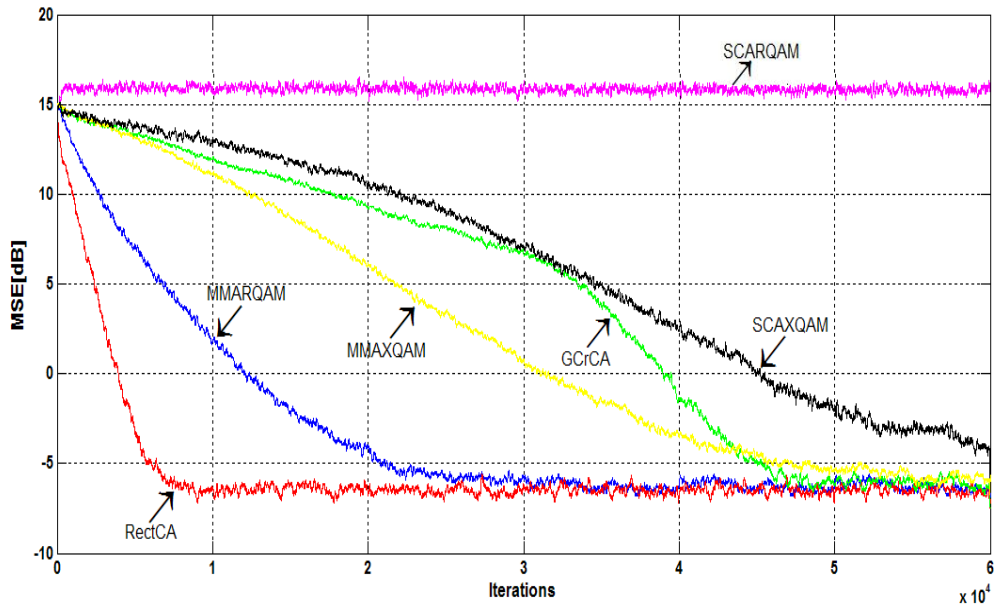


Fig.4.9 MSE traces for 128-XQAM and 128-RQAM (1.75 distance b/w symbols)

Conclusions and Future Work

In this thesis, Rectangular QAM is analyzed and mathematical expressions for average energy, minimum distance d_{\min} and symbol error probability (SEP) over AWGN and fading channels including Rayleigh, Nakagami-m, Nakagami-q (Hoyt) and Nakagami-n (Rice) are derived. A family of new blind equalization algorithm for rectangular QAM constellations namely Generalized Rectangular Contour Algorithm has been proposed. The proposed algorithm gives fast convergence rate and low mean squared error than those of its counterparts proposed for both cross and rectangular QAM constellations to accommodate the transmission of odd number of bits. The reason for this better performance is that GR_{RECT}CA generates a rectangular zero error contour which is in match with the shape of the constellation and ability of the rectangular constellation of correcting any phase error within 180 degrees in contrast to cross and square QAM constellations which correct the phase error up to 90 degrees. Moreover, the rectangular zero error contour of the proposed algorithm can be modified to square zero error contour by mere change of two constellation dependent constants a and b . As a result the algorithm can be used in equalizing both rectangular and square QAM constellations facilitating the transmission of even and odd number of bits in any communication system. Simulation results for 32 and 128 QAM constellations validate the effectiveness of the proposed blind equalization scheme over SCA, GCrCA and MMA for non-square constellations.

This improved performance calls for the modification of other blind equalization using Rectangular QAM. The modification of the proposed algorithm can also be done by bring the decision device output into the cost function as done in case of Improved SCA.

Finally, all the modifications done on SCA as (Modified-SCA, Constellation Matched-SCA, Improved-SCA, Modified Constellation Matched-SCA) can be done on the proposed algorithm to further improve the performance in terms of low steady-state error and fast convergence rate.

REFERENCES:

- [1] G.H. Im, D.D. Harman, G.Huang, A.V. Mandzik, M.H.Nguyen, and J.J. Werner, "51.84 Mb/s 16-CAP ATM-LN standard," *IEEE Journal on Selected Areas in Communication*, vol.13, pp.620-632, May 1995.
- [2] G.H. Im and J.J Werner, "Bandwidth-efficient digital transmission over unshielded twisted pair wiring," *IEEE Journal on Selected Areas in Communication*, vol.13, pp.1643-1655, Dec 1995.
- [3] D.D. Harman, G.Huang, G.H.Im,M.H.Nguyen,J.J.Werner, and M.K.Wong, "Local distribution for IMIV," *IEEE Multimedia*, vol.2, pp.14-23, Fall 1995.
- [4] J. G. Smith, "Odd-bit quadrature amplitude-shift keying," *IEEE Transactions on Communications*, vol. 23, no. 3, pp. 385–389, 1975.
- [5] Jenq-Tay Yuan and Kun-Da Tsai "Analysis of the multi modulus blind equalization algorithm for non-square rectangular QAM signal constellations" ICSF'04 Proceedings
- [6] Shafayat Abrar "A New Cost Function for the Blind Equalization of Cross-QAM Signals"
- [7] John Cioffi, *Advance Digital Communication*,
- [8] N. C. Beaulieu, "A useful integral for wireless communication theory and its application to rectangular signaling constellation error rates," *IEEE Transactions on Communications*, vol. 54, no. 5, pp. 802–805, 2006.
- [9] A. Maaref and S. A`issa, "Exact error probability analysis of rectangular QAM for single- and multichannel reception in Nakagami-m fading channels," *IEEE Transactions on Communications*, vol. 57, no. 1, pp. 214–221, 2009.
- [10] X. Lei, P. Fan, and Q. Chen, "On the average of the product of two Gaussian Q-functions over Nakagami-q (Hoyt) fading and its application," *IEEE Communications Letters*, vol. 11, no.10, pp. 805–807, 2007.
- [11] M. Simon and M.-S. Alouini, *Digital Communication over Fading Channels*, JohnWiley & Sons, New York, NY, USA, 2nd edition, 2005.
- [12] M. K. Simon, "Some new twists to problems involving the gaussian probability integral," *IEEE Transactions on Communications*, vol. 46, no. 2, pp. 200–210, 1998.
- [13] M. K. Simon, "A simpler form of the craig representation for the two-dimensional joint Gaussian Q-function," *IEEE Communications Letters*, vol. 6, no. 2, pp. 49–51, 2002.
- [14] G. T. F. De Abreu, "Jensen-cotes upper and lower bounds on the Gaussian Q-function and related functions," *IEEE Transactions on Communications*, vol. 57, no. 11, pp. 3328– 3338, 2009.
- [15] A.H.Syed, "Fundamentals of Adaptive Filtering," Published by Wiley-IEEE,2003
- [16] Y.Sato, "A Method of Self-Recovering Equalization for Multilevel Amplitude Modulation Systems," *IEEE Trans on Comm*. 1975.
- [17] D.Tse, P. Viswanath, "Fundamentals of Wireless Communications," Published by Cambridge University Press, 2005. pp.29-35.

- [18] T.S.Rappaport, "Wireless Communications: Principles and Practice," Prentice Hall, 2002.
- [19] T.Thaiupatump, S.A.Kassam, "Square contour algorithm: A new algorithm for blind equalization and carrier phase recovery", in Proc. 37th Asilomar Conference on Signals, Systems and Computers, 2003, pp.647-651
- [20] K. Wesolowski. "Self-Recovering Adaptive Equalization Algorithms for Digital Radio and Voiceband Data Modems". Proc. European Conf.Circuit Theory and Design, pages 19-24, 1987.
- [21] K. N. Oh and Y. O. Chin. "Modified Constant Modulus Algorithm: Blind Equalization and Carrier Phase Recovery Algorithm". Proc. IEEE Int. Conf Commtn.,1:498-502, June 1995.
- [22] J. Yang, J. J. Werner and G. A. Dumont. "The Multimodulus Blind Equalization Algorithm". Proc. IEEE Intl. Conf DSP, 1:127-130, 1997.
- [23] J. Yang, J. J. Werner, and G. A. Dumont. "The Multimodulus Blind Equalization and its Generalized Algorithms". IEEE Jr Selected Areas Commun.20(5):997-1015, June 2002.
- [24] J. Yang. "Multimodulus Algorithms for Blind Equalization". PhD thesis, University of British Columbia, Aug. 1997.
- [25] Xi-chun Zhang, Hua Yu, and GangWei "Exact Symbol Error Probability of Cross-QAM in AWGN and Fading Channels"
- [26] Victor Demjanenko Ph. D., Paul Marzec MS, and Alberto Torres Ph.D. IEEE P802.15 Working Group for Wireless Personal Area Networks (WPANs) "Reasons to use non-squared QAM constellations with independent I&Q in pan systems" IEEE P802.15-15-03-0311-00-003a.
- [27] J.Mai, A.H. Sayed, A feed backs approach to the steady-state performance of fractionally spaced blind equalizers, IEEE Trans. Signal Process. 48(1)(2000) 80-91
- [28] L.He, Improved blind equalization algorithms and analysis, Ph.D.thesis, University of Pennsylvania,2005.

